UNIVERSITY OF TURKU

Effect of Gating Design on Melt Flow Velocity in Gravity Sand casting using AM-Enabled Molds

Metal Casting

Master's Degree Programme in Mechanical Engineering

Department of Engineering, Faculty of Technology

Master of Science in Technology Thesis

Author:

Umar Siddique

Supervisors:

Dr. Sampsa Laasko (University of Turku)

Dr. Kalle Jalava (Tampere University)

June 2025

Master of Science in Technology Thesis
Department of Engineering, Faculty of Technology
University of Turku

Subject: Sand Printing and Metal Casting
Programme: Master's Degree Programme in Mechanical Engineering
Author: Umar Siddique
Title: Effect of Gating Design on Melt Flow Velocity in Gravity Sand Casting using AM-enabled molds
Number of pages: 60 pages
Date: June 2025

This research thesis deals with the effect of gating design on melt flow characteristics in sand casting. Different gating designs have been studied by varying the number of ingates and prospective benefits of AM-enabled molds to design these filling systems has been noted. This thesis focussed on simulation work conducted on casting using flow3dcast software. The ingates is the portion of the mold which connects the filling system to mold cavity. The goal of the thesis was to find out if it was feasible to increase the number of ingates while increasing the metal input rate. This would lead to faster filling of the mold. Filling simulation was performed for 3 different cases using one ingate, 2 ingates and 4 ingates. A test case simulation was also performed with alternate filling system. 2 filling systems were considered, conventional system composed of conical basin, tapered sprue and a sprue well and alternate system composed of offset basin, tapered sprue and curved connection to runner. The results showed that the filling time can be reduced from 7 seconds in case of single ingate to 3.5 seconds with 4 ingates using a conventional filling system, , while minimizing the air entrapment in mold cavity. This showed that increasing the number of gates from 1 to 4 reduced the filling time to half and this would could eventually lead to doubling the production rate of foundries.

Keywords: melt, flow, velocity, ingates, casting, sprue, runner, basin.

Table of contents

1 Introduction

1.1 Background

Metal casting has been a fundamental manufacturing technique since ancient times and continues to play a crucial role in modern production. Traces of oldest remains of metal casted parts have been found from Indus Valley Civilization and is estimated to be 6000 years old. For example one model was obtained from Mohenjo-Daro from modern day Pakistan, made of copper alloy utilizing the lost wax technique. Other objects like tools, weapons and even currencies were found developed using metal casting. Ancient Mesopotamia introduced two types of lost wax methods, known as direct method utilizing hands and tools for molding while the indirect method uses molds and thus remained to be the popular because of intricate shapes that can be achieved. [1]

Metal casting plays a huge role in today's modern day metal manufacturing industry. According to Precedence Research statistics metal casting is calculated at USD 199.86 billion in 2025 and is estimated to reach USD 400.74 billion by 2034. [2] That is almost getting double in a period of decade. From large scale parts like automotive engine casings and ship components to intricate parts like jewellery, dental tools, are made using this process. Metal casting has been an irreplaceable manufacturing operation even with advent of modern metal additive manufacturing techniques.

The casting process of metal is performed using different approaches. The most standard and basic approach is sand casting where molten metal is poured into the sand mold and after the certain time period it solidifies and it is taken out of the mold. This thesis is mainly focussed on utilization of sand casting. The other common approaches to cast a metal is through die casting which further categorizes into High Pressure Die Casting (HPDC) and Low Pressure Die Casting (LPDC). Investment casting is one of the oldest and prominent form of casting used in central asia for ages. This includes Lost-wax casting, lost-foam casting and lost-PLA casting. Vacuum casting, centrifugal casting, squeeze casting are some of the other types.

Casting can be performed for pure metals as well as alloys. Mostly industrial casting is focussed on alloy casting. Grey cast iron is the most common used alloy in foundries. Aluminum alloys like A356, AlSi10Mg and numbers of other are commonly casted. Steel is another most common alloy casted requiring extremely high melt temperatures. A number of properties can be achieved with steel like hardness by adding Boron and Manganese or increasing the ductility

by adding titanium in small amounts. Further phase composition can be manipulated by controlling the cooling rates and that also gives different properties of steel.

Now-a-days casting simulation has given industries much needed freedom to design new molds and test different filling systems for research. A number of software have been launched for example Flow3dCast, ProCast, Magmasoft etc., which can give very accurate results for casting in very less time. These software have paved the way for other new techniques such as development of additive manufacturing enabled sand molds. These simulations model the entire casting process — including mold filling, solidification, cooling, and defect prediction — allowing engineers to optimize gating design, feeding systems, and process parameters before physical trials. This virtual prototyping reduces trial-and-error iterations, saving both time and material. From an environmental standpoint, casting operations are resource-intensive, involving high energy consumption and emissions. Poorly optimized castings lead to material waste, excessive energy use, and increased carbon footprint. By minimizing defects and improving yield, casting simulations contribute to more sustainable manufacturing, reducing the environmental impact per component produced.

1.2 Motivation

In modern times, casting process is being carried out on an extensive scale around the globe from small-scale manufacturing units to bigger foundries. Still to this date, casting operations mostly rely on the hit-and-trial approach devised by experienced foundry-men. This leads to a lot of metal being wasted. In sand casting, traditional mold making process requires the addition of binders and this needs to be baked at high temperature leading to the release of dangerous pollutant gases containing Volatile Organic Compounds (VOCs). A number of research articles have been directed towards the poor health quality of foundry workers. As the metal is poured into the sand mold, the binder burns into the air releasing harmful toxins. In some cases, the fumes needs to be vented out through equipment such as blowers or fans. Furthermore, casting design needs several improvements to develop defect-free castings. Flow turbulence and air entrapment are some of biggest issues that needs to be avoided. Turbulence is caused when a liquid metal flow at a high speed resulting in air getting entrapped in the liquid metal. Metal pouring velocity, height of drop, pouring basin design, sprue design, gating and runner design are some of the factors influencing the casting quality. The problem with the traditional sand mold design is that we cannot adjust these parameters properly as there is not much design freedom. With the advent of modern additive manufacturing operations, sand molds can be

additively manufactured with precise details and thus providing increased design freedom. For example it has been shown over and over again that parabolic and conical sprues are better than straight sprues for defect prevention simply because the laminar metal flow is ensured. This avoids oxide formation and hence reduces porosity and cracks. In traditional mold making, straight tapered spures can be made while it is nearly impossible to make a parabolic or conical sprues. Most of the small-medium scale foundries are unaware of the usage of computational tools used for simulation of casting process. The software can effectively predict the filling time, turbulence, solidification time, stress concentration etc. using a system of algorithms. This saves time, energy and cost in developing a new casting prototype only to find out that it is failed. This thesis would target the casting analysis using computer simulations. Verification could be done with best designs using experimental approach.

Filling time is an important parameter for casting industries to gauge the production time and efficiency. Faster filling time would ultimately lead to greater production rate and greater profits. Having the ability to produce defect-free casting at a higher production rate is the objective of casting industries. One of the many techniques employed is the use of multi-gating system that allows the filling of molds at quicker rate. With multiple gates the volume flow rate of the entry metal can be increased while still keeping the flow under the critical velocity limit of 0.5 ms^{-1} at the ingates [3]. Since the volume flow rate, molds can be filled quicker thus increasing the production rate.

1.3 Objectives

The goal of the research is to study the effect of filling system on the final quality of castings developed using aluminium alloy AlSi10Mg. The specific focus in this research would be to study various gating system designs. The goal would be to verify if the filling time could be increased by increasing the number of gates and still maintaining the quality of final part achieved through this process. Simulation analysis would be performed using Flow3dcast software and solidification analysis would be used to look for defects especially porosity, entrapped air bubbles, cracks, tears etc. Sprue design is important as this component guides the liquid metal into the mold cavity. Major forms of defects including porosity, oxide cracks, tears etc., in casted parts are a consequence of poor sprue design. The study focusses on utilization of additive manufacturing of sand molds as a means to develop complex filling geometries like multiple branched runners. One of the important design considerations is ensuring the laminar flow of liquid metal while keeping the filling time as low as possible. A quicker filling operation

leads to lesser solidification time and hence less shrinkage. The approach used in this study would be to determine the melt flow velocity at the end of the runner, while comparing different runner combinations. The viability of offset basin in reducing the air influx would be noted.

1.4 Scope

This thesis entails the study of effects of multi-gating system on filling time for gravity sand casting. The filling system consists of multiple components such as pouring basin, sprue, runner, filters, ingates, feeders etc. Most of the literature has been directed towards the efficient sprue design and pouring basin. Very little literature is directed towards multi-gating system for gravity sand casting. Currently with the utilization of additive manufacturing of sand molds, it has been proven that filling system and mold system of relative complexity can be made easily without any challenges like expensive tooling. Complex gating system with multiple gates can be developed at much faster speeds than ever before using additive manufacturing. This research will show how the runner with multiple gates developed using additive manufacturing is more efficient in filling mold cavity while minimizing filling time and producing defect-free casting. This work would only entail simulation work using flow3dcast software. Further verification would be needed to perform using experiments.

1.5 Thesis Organization

This is a master's level thesis in mechanical engineering related to metal casting. The thesis starts with basic background of the topic on sand casting. It sheds some light on the history of casting, then describes the motivation and scope of the research work presented. The second chapter introduces some fundamental concepts related to sand casting. Also it enlists the various computational methods to simulate the flow. The third chapter describes in detail the relevant literature on metal casting of aluminium alloys. It also describes of the current work on gating design, gating ratios, oxide and bifilm formation in castings. Chapter 4 introduces about the research methods used in the study including simulation model setup using Flow3dCast. Chapter 5 describes in detail about the simulation results and discussion and last chapter briefly concludes the thesis and enlists the major findings.

2 Fundamentals of Casting and Casting Simulations

Throughout the ages, metal casting has gone through several changes and with the advent of modern computational approach, casting operation has become simpler. Computational techniques are utilized to predict the defects in various cast regions which improves the chance of achieving a good quality cast. The basic process of metal casting involves having a liquid metal preferably free from impurities like oxides and other trace elements. This liquid metal is poured into the mold containing the pattern of the part intended to be casted. The sand is first filled in the metal or wooden casing known as flask, which has two sections separated by a parting line in the middle. The top section containing half of the mold cavity is known as cope and the bottom half is known as drag. The two sections are held in place using locating pins. The liquid metal is poured through the gating system into the mold cavity. Gating system include pouring basin, runner, sprue and gates. The goal of the gating system is to direct the metal into the mold cavity. The risers are kept in the system to compensate for the shrinkage as the metal cools down. The extra metal can then be removed from the mold. The mold cavity contains a core which is an insert to produce internal features in the casting part. Vents are also provided to remove the gases generated during the process. A good practice is to keep a draft when making a mold, so that mold can be easily taken off after the process. [4] The Figure 1 below shows the pictorial representation of terms used in casting.

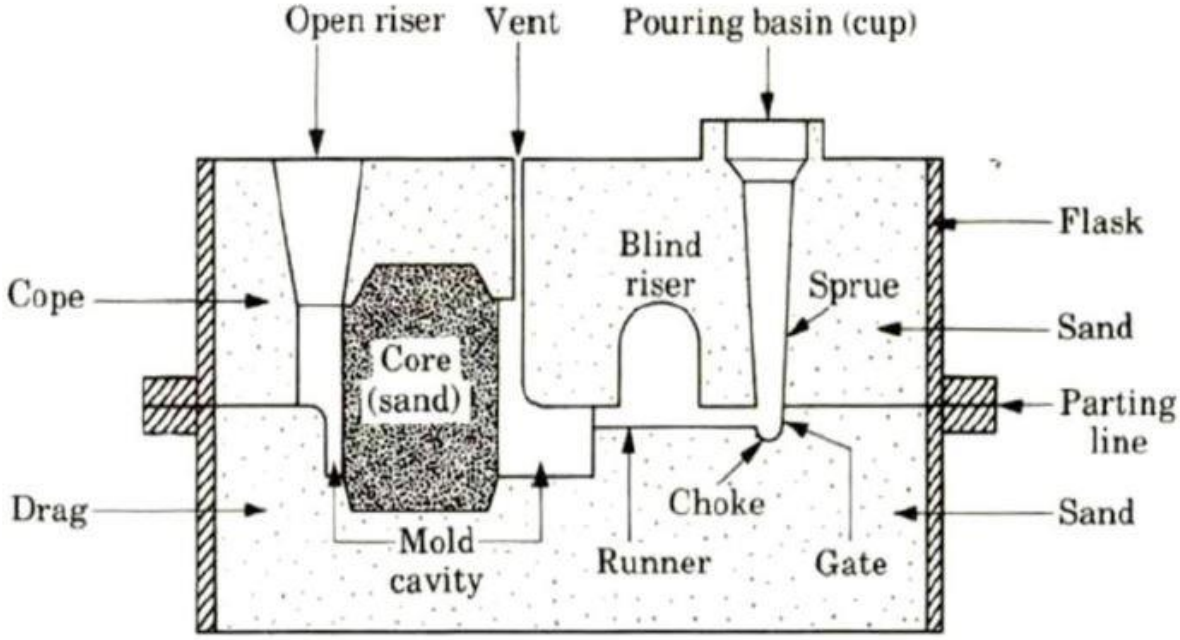

Figure 1 Diagram illustrates a sand casting mold, showing the flow of molten metal from the pouring basin through the sprue, runner, and gate into the mold cavity. Picture: Osama Mohammed [5]

2.1 10 Rules of Metal Casting

John Campbell suggested that in order to define a good quality casting, there are 10 rules which needs to be followed and failure to follow one of the rules could lead to damaged final product.[3] These rules are detailed below along with relevant literature.

2.1.1 Use of Good Quality Melt

Use of good quality melt is absolutely paramount in achieving a high quality casting. Melt is typically the first step to initiate the casting. During melting there is a significant risk of air entrapment resulting in oxide formation in aluminum alloy. One study by Gyarmati et al., from 2022 studied the effect of grain refiner settling on the melt quality of aluminum casting alloys. The experimental study was directed at finding the effect of Ti Concentration on the melt quality of Al-Si-Mg-Cu alloy. This was achieved by the introduction of blocky Al_3Ti which re-precipitated in the form of $(AlSi)_3Ti$. The settling of $(AlSi)_3Ti$ improved the melt quality and better sedimentation of bifilms in the melt was achieved.[6]

A new study suggested by Toni Bogdanof found a simple procedure to assess the complete melt quality for aluminum castings. The study utilized the use of Reduced Pressure Test (RPT) and tensile testing at various instances from furnace to the production line. Two case studies were performed for aluminum die casting and rheo casting consecutively, and it was found that melts get significantly damaged in tower furnace and the quality gets worsened in subsequent steps of production process. This was determined using RPT, tensile testing and fracture surface analysis.[7]

2.1.2 Avoid Turbulence during metal pouring

After good quality melt is achieved, some of the problems related to bifilms are linked to the introduction of melt into the mold cavity. To avoid turbulence during metal pouring, one important aspect is the passing of melt through gating system. Melt should always be introduced in the uphill motion into the mold against the gravity, this allows the bifilm layer to remain on the top near meniscus and avoids the entrapment of bifilms into the metal. [3]

Air entrapment is one of the major problems during metal casting process, which leads to porosity and thus becomes a hindrance in achieving a superior-quality castings. Turbulent flow of liquid metal into the mold leads to air entrapment. One study conducted by Samir Chakravarti used Computational Fluid Dynamics (CFD) based approach to determine the relation between

casting parameters and porosity and to estimate the casting parameters with minimum porosity. The study investigated the relationship of porosity with pouring temperature and pouring velocity. Casting process of pure Al (99% approx.) was simulated using ANSYS Fluent. The metal filling and solidification model of transient flow gravity casting were studied by the two-phase volume of fluid method (VOF model). It was found that the top surface of the casting had the maximum porosity with porosity was observed to be extremely low when the pouring velocity was 500 mm/s (0.5 m/s). [8] This was re-assured as determined by John Campbell in earlier study. [3]

2.1.3 Avoid Laminar Entrainment

As the liquid metal is introduced into through the gating system, a meniscus if formed on the liquid front. Ideally, the meniscus should move in a steady manner while staying on the surface and expanding continuously at all points. This can be achieved by the utilization of counter-gravity gating system, as it would avoid the liquid metal to reach turbulent speeds as discussed in previous section. Now the problem arises if the liquid melt speed is too low and bifilm is formed on the liquid front inhibiting the flow of further melt. This liquid bifilm can become strong and rigid which would make the liquid overflow and a new film would be formed over the existing layer. This is what is known as an oxide lap and is commonly observed in the castings as crack. To avoid this sudden increase in melt flow cross-section needs to be avoided. Further this problem could arise if some of the metal leaks creating a waterfall effect, thus avoiding the further expansion of the meniscus and allowing the bifilm to be solidified. [3] The Figure 2 below illustrates the formation of lap defect.

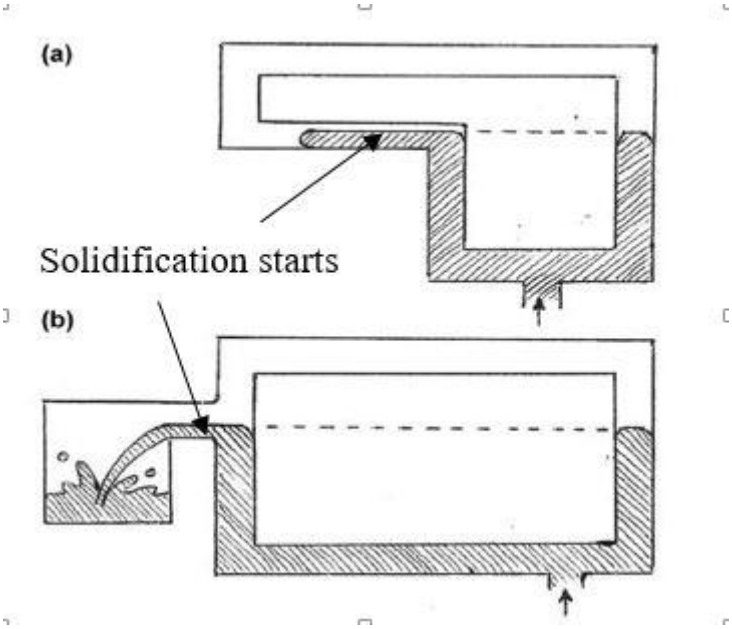

Figure 2 Diagram showing two filling situations showing the advance of melt and highlighting the areas from where solidification can start and introducing lap defects (a) enlarged area (b) waterfall effect stops the advance of melt front. [3] Picture: John Campbell

A study conducted by A. H. Fazeli and colleagues studied the fluidity and effective surface tension of Al-Ductile Iron at different pouring temperatures. It was found that by increasing the concentration of Al in the melt results in the formation of alumina film on the liquid front which increases the surface tension and also results in the difficulty of metal to reach the tighter sections of the mould ranging from 0.4-1.0 mm. [9]

2.1.4 Avoid Bubble Entrapment

Bubble entrapment happens when the oxide bifilms produced has air entrapped inside and most of porosity because of this phenomena. These bubbles in the liquid melt could lead to the formation of bubble trails, which can remain inside the melt even after the bubbles have been removed. This problem commonly occurs due to poor design of the feeding system. The bubbles can be formed at any step of the process starting from liquid melt falling from the pouring cup, passing through the gating system or entering the mould cavity. This problem can be avoided in gravity assisted casting by the proper sprue design. Tapered design of sprue is recommended as this causes the cross-section of the liquid to reduce as it enters the mold cavity, this lowers the chance of the bubbles being formed melt. On the other hand, straight and negative tapered design of the sprue leads to this issue. One of the study carried out by Rafal Dojka used MagmaSOFT to determine the effect of different sprue designs on the formation of bubble in the bifilms. Nine different design of sprue were proposed and analysed using the

software. It was found that tapered sprues are preferable over the straight ones. In case of hyperbolic tapering, 60% increase in yield was observed. Further rectangular sprues improves the flow kinetics by reducing the flow entrainment in bends and greater friction causes the flow to move in a steady manner compared to round sprues. [3]

Counter-gravity casting system is more suitable to avoid bubble formation if the pumped system is used as utilized in low pressure casting. Since the entire system is pressurized a minor leak in any of the sections for example in the riser could potentially lead to the inclusion of air into the system and can ruin the casting result. Thus this needs to be avoided at all costs. [3]

2.1.5 Avoid Core Blows

Core blows happen as a result of reaction of liquid metal with some constituents within core such as traces of water. This could result in an explosive reaction causing the water to evaporate and condense on any cooler surface as the melt cools down. This would result in the formation of pits on the metal surface and thus damage the final cast. In order to avoid this issue, proper measures should be taken to dry the sand very well through. Further the chill should be covered with ceramic coating, thoroughly dried to give permeable non-wetted surface. Additionally, vents should be kept in the mold core and the top-most portion of the core to allow the gases to escape. [3]

2.1.6 Avoid Shrinkage Damage

A recent study by Yizhou Xiao determined a control method to reduce shrinkage defects in investment casting using a time varying disturbance in temperature field. It was observed that during the transfer process of shell from pre-heating furnace to pouring furnace the temperature drops a lot resulting in major shrinkage and total defects. Both numerical simulation and practical site measurements were taken for this purpose. Results showed that as the time is varied from 0 to 240s the surface temperature dropped from 950 C to 776 C leading to 512.34% increase in shrinkage defects and 285.47% rise in total defects. The results were then compared by using time varying temperature control method and insulating the shell using various methods kept temperature above 930 C and resulting 83.67% reduction in shrinkage and 90.18% in total defect volume. [10]

2.1.7 Avoid Convection

Convection happens as a result of liquid metal flowing inside the mould due to either filling or feeding. As the liquid metal flows, the hot metal rises to the top portion of the mold which solidifies and the system becomes stable. If the slight changes happen either by filling or feeding, the solidified portion might become unstable and move down causing the newly added hot metal to rush to the top, this creates a convective loop and can result the castings to fail miserably. To avoid this problem, feeding needs to be done from the top, that will keep the hot metal to the top where it will remain due to being of lower density. Secondly, this problem can be avoided by either keeping the solidification time too low, preferably less than 1 min to avoid convection to start in first place. The second option here is to keep the solidification time high, preferably above 10 minutes to settle down everything and making the system stable. Furthermore, this problem can be avoided by keeping thin sections in casting design as it will prevent the metal to flow freely. [3]

2.1.8 Reduce Segregation

Segregation can be divided into 2 different categories microsegregation resulting from localized freezing of dendritic arms and macrosegregation happens as a result of slow cooling of casting resulting in channel defects. Microsegregation is not a big problem in Al alloys but alloys containing copper content can face such issues. To avoid this problem, a general and recommended strategy is to reduce the cooling time. Secondly, additional chills should be used along the temperature gradient to avoid abrupt temperature changes. [3]

2.1.9 Reduce Residual Stress

Residual stress can develop in castings as a result of variety of reasons related either to casting parameters or part geometry. To reduce the residual stress in casting, heat treatment in recommended after casting process. The process is done by heating the casted part to sufficiently high temperature known as stress-relief temperature to remove any unwanted stress. The castings are put into the furnace and temperature is made to rise gradually to the stress-relief temperature. Different alloys have different stress-relief temperature e.g., for aluminum the temperature is 300 C. It has been shown that 100% of the stress can be eliminated by one hour at the stress relief temperature for most alloys. [3]

2.1.10 Provide Location Points

This rule emphasizes the importance of incorporating clear, defined reference features—known as location points or datums—into the casting design. These points act as consistent and repeatable references for machining, inspection, and assembly processes. Without proper datums, downstream operations may suffer from alignment errors, increased variation, and reduced dimensional accuracy. Well-placed datum pads, bosses, or holes help ensure the part is properly oriented in fixtures and tooling. For maximum effectiveness, these features should be located in low-distortion areas of the casting. Incorporating good location points ultimately improves manufacturing efficiency, product quality, and assembly reliability. [3]

2.2 Use of Computer Simulation Technique in Metal Casting:

Computer simulations have been used in metal casting since the 1960s as a means to determine the quality of the final cast part. The numerical simulations are carried out to determine the properties of filling flow and solidification process in mold. The objective of the casting simulation is to predict the formation of the defects in the casting such as pores formation, shrinkage, tears, hot cracks etc. These defects can be avoided with the proper implementation of casting parameters as obtained from the numerical simulation techniques. Ensuring the adherence to casting parameters would inevitably lead to better manufactured parts, improved surface quality, reduced defect formation and thus increasing the yield of the product. Casting simulations have been divided into various domains such as temperature simulation, pressure simulation, flow simulation and microstructure simulation. For the scope of this thesis we will discuss solidification and filling simulation here. Most of the literature can be found related to these simulation types.

2.2.1 Solidification Simulation:

As the liquid metal is introduced into the mold, it gradually releases the heat to the surrounding mold which reduces its temperature and it solidifies into the shape of the mold. Different heat transfer process takes place in the mold such as heat conduction between casting and surrounding mold, heat radiation between casting and surrounding environment and convective heat transfer within the liquid metal. The solidification simulation also computes the latent heat of solidification released to covert the molten liquid metal to solid. Furthermore, the simulations involves the temperature field analysis to determine the rates of cooling. Also the shrinkage and porosity during the solidification process is predicted. [11,12]

Solidification simulation uses the Finite Difference Method (FDM) approach to solve the heat conduction during solidification as this approach solves partial differential equations (PDEs) by discretizing a continuous domain into a grid (mesh) of points. Each grid point represents a discrete approximation of the solution. This is especially useful for heat transfer problems in solids as the geometry and mesh are fairly regular and this approach reduces the complexity of the computation. The general 3D heat conduction equation in spatial co-ordinates with a heat generation term is given as follows.

$$\frac{\partial \mathrm{T}}{\partial \mathrm{x}} = \alpha\left(\frac{\partial^2 \mathrm{T}}{\partial \mathrm{x}^2} + \frac{\partial^2 \mathrm{T}}{\partial \mathrm{x}^2} + \frac{\partial^2 \mathrm{T}}{\partial \mathrm{x}^2}\right) + \frac{\mathrm{q}}{\rho \mathrm{c_p}} \quad (1)$$

Where,

T(x,y,z,t) = Temperature (°C or K)

t = Time (s)

x,y,z = Spatial coordinates (m)

$\alpha = \frac{q}{\rho c_p}$ *= Thermal diffusivity (m²/s)*

k = Thermal conductivity (W/m·K)

ρ = Density (kg/m³)

c_p *= Specific heat capacity (J/kg·K)*

q = Internal heat generation per unit volume (W/m³)

2.2.2 Filling Simulation

As the liquid metal is poured into the mold it flows through the gating system, sprue, runners etc before reaching the mold cavity. This process includes the variety of instances which leads to defect formation in the latter casting as discussed by the John Campbell such as laminar entrainment, turbulent entrainment, bubble entrainment, oxide bi-film production. The flow of liquid metal is accompanied with velocity, temperature and pressure changes and thus the numerical computation becomes intensive. This is due to the fact that Navier-Stokes (N-S) equation needs to be implemented to simulate a fluid flow including the N-S momentum

equations. The high temperature liquid metal is generally considered as unsteady viscous incompressible Newtonian fluid.[13]

Mass Conversation Equation,

$$\frac{\partial u}{\partial x}+\frac{\partial v}{\partial y}+\frac{\partial w}{\partial z}=0 \tag{2}$$

Navier Stokes Equation given in 3 spatial co-ordinates and time co-ordinate are given as follows in the form of 3 equations each representing the flow in x, y and z co-ordinates.

$$\rho\left(\frac{\partial u}{\partial t}+u\frac{\partial u}{\partial x}+v\frac{\partial u}{\partial y}+w\frac{\partial u}{\partial z}\right)=-\frac{\partial p}{\partial x}+\rho g_x+\mu\nabla^2 u \tag{3}$$

$$\rho\left(\frac{\partial v}{\partial t}+u\frac{\partial v}{\partial x}+v\frac{\partial v}{\partial y}+w\frac{\partial v}{\partial z}\right)=-\frac{\partial p}{\partial y}+\rho g_y+\mu\nabla^2 v \tag{4}$$

$$\rho\left(\frac{\partial w}{\partial t}+u\frac{\partial w}{\partial x}+v\frac{\partial w}{\partial y}+w\frac{\partial w}{\partial z}\right)=-\frac{\partial p}{\partial z}+\rho g_z+\mu\nabla^2 w \tag{5}$$

Energy Conservation,

$$\frac{\partial\left(\rho c_p T\right)}{\partial t}+u\frac{\partial\left(\rho c_p u T\right)}{\partial x}+v\frac{\partial\left(\rho c_p v T\right)}{\partial y}+w\frac{\partial\left(\rho c_p w T\right)}{\partial z}$$
$$=k\left(\frac{\partial^2 T}{\partial x^2}+\frac{\partial^2 T}{\partial x^2}+\frac{\partial^2 T}{\partial x^2}\right)+S \tag{6}$$

Where,

u, v and *w* are fluid velocities in x, y and z directions.

g_x, g_y and g_z are gravitational acceleration in x, y and z directions.

∇^2 is the Laplace Operator

ρ is density, p is pressure, T is temperature, μ is kinematic viscosity, c_p is specific heat capacity at constant pressure.[13]

This process is done by the implementation of k-epsilon (k- ε) turbulent model to solve mass, momentum and energy conversation. This model is used for prediction of defects caused by turbulence such as air entrapment and oxide bi-film production. This is a two equation turbulence model that solves turbulent kinetic energy (k), showing the intensity of turbulence and turbulent dissipation rate (ε) shows the rate of dissipation of turbulent kinetic energy into internal energy (heat). [13] The equations are turbulent kinetic energy equation (k) and turbulent dissipation rate equation (ε) correspondingly given below as,

$$\frac{\partial k}{\partial t} + U_j \frac{\partial k}{\partial x_j} = \frac{1}{\rho}\frac{\partial}{\partial x_j}\left[\left(v + \frac{v_t}{\sigma_k}\right)\frac{\partial k}{\partial x_j}\right] + P_k - \epsilon \tag{7}$$

$$\frac{\partial \epsilon}{\partial t} + U_j \frac{\partial \epsilon}{\partial x_j} = \frac{1}{\rho}\frac{\partial}{\partial x_j}\left[\left(v + \frac{v_t}{\sigma_k}\right)\frac{\partial \epsilon}{\partial x_j}\right] + C_1 \frac{\epsilon}{k} P_k - C_2 \frac{\epsilon^2}{k} \tag{8}$$

Where,

U_j = velocity component in the j-direction.

ν = Kinematic viscosity.

ν_t = Turbulent viscosity ($\nu_t = C_\mu \frac{k^2}{\epsilon}$) .

P_k = Turbulence production term.

$C_1, C_2, C_\mu, \sigma_k, \sigma_\varepsilon$ = Model constants.

Some of the most widely used simulation algorithms used for casting filling process by computational software are as follows.

- **SIMPLE Algorithm:** The SIMPLE (Semi-Implicit Method for Pressure-Linked Equations) method was introduced by S.V. Patankar and D.B. Spalding in 1973. [14] This method uses an iterative approach to solve Navier-Stokes equation by correcting pressure and velocity fields and the process is repeated till convergence is achieved. This algorithm is only limited for incompressible flows and has extremely slow convergence for high Reynolds number flows.

- **MAC and SMAC Algorithm:** The MAC (Marker-And-Cell) method was first introduced by Harlow & Welch in 1965 as finite difference method to solve incompressible flow using staggered grid approach by storing flow velocities at cell faces and pressure at cell centers. Since the velocity and pressure fields are needed to be simulated simultaneously, this results in large calculation with low efficiency. SMAC (Simplified MAC) is an improved version of the MAC Algorithm with a predictor-corrector step to enhance stability and accuracy. [15]

SOLA-VOF Algorithm: The SOLA-VOF (Solution Algorithm – Volume of Fluid) method was first developed by Hirt and Nichols in 1981. This is most widely used numerical simulation algorithm used in casting filling simulation. The algorithm consists of two parts, SOLA method is used to determine the momentum and continuity equation while VOF method is used to determine volume function F which represents free surface. Volume function is given as:

$$\frac{\partial F}{\partial t} + \frac{\partial Fu}{\partial x} + \frac{\partial Fv}{\partial y} + \frac{\partial Fw}{\partial z} = 0 \tag{9}$$

Where,

F is the volume function; $0 \leq F \leq 1$

This approach considers the fluid unit and volume function is applied on each of the unit to determine the position and shape of the free surface of the liquid inside the fluid unit. When the unit has no liquid, $F=0$. When the unit is filled $F=1$, for $0 < F < 1$ the fluid unit has free surface. This algorithm is considerably fast, efficient and stable and hence mostly used for filling simulation. [16]

3 Literature Review

3.1 Additive Manufacturing of Sand Molds:

Sand 3D printing is an additive manufacturing process which uses binder jetting technology to bind sand particles in layers to generate a mold for metal casting process. The process works with layer by layer deposition of the sand particles and subsequent heating of the layer which is also called interlayer curing. These steps are repeated to form a 3D shape of the mold using the design file provided by the software. After the mold is prepared, it is removed from the machine and cleaning of excess powder is done using a fine brush. The mold is then cured under heat to making it appropriate to handle high temperatures of liquid metal. [17]

The main objective of sand 3D printing is to generate highly intricate mold and core geometries while significantly reducing lead time. This proves highly cost-effective for foundries aiming to develop multiple cast parts in less time. Sand 3D printing offers some promising benefits to foundries such as reduced lead time, faster prototyping and ability to produce complex and intricate geometries with very high accuracy as compared to traditional mold making process. [18]

3.2 Benefits of Additive Manufacturing in Sand Mold Design:

Most of the foundries in Finland rely on traditional methods of mold making to generate metal casting components causing VOCs (Volatile Organic Compunds) emissions and pollution. [19] With the introduction of sand 3D printers the yield of the foundries can be significantly improved. Some of the benefits of sand 3D printing are summarized below with reference to relevant research in the corresponding domains.

3.2.1 Reduced Lead Time

Sand printing can be used to improve the mold design by the improvement of significant features of the casting mold which can lead to effective reduction in lead time.

3.2.2 Improved Casting Quality

3D Sand Printing (3DSP) has been shown to improve the casting quality due to high precision and accuracy of mold making.

3.2.3 Cost Savings:

- **Determination of Complexity factor:**

One of the first steps to determine the cost savings of the 3D sand printing is to quantify the role of complexity so to find out when is it feasible to use 3D printing. This work has been done by a lot of researchers in the past [20–26]. One of the interesting and detailed analysis was carried out by Eyad S. Almaghariz from Youngstown State University in 2015. The study was carried out to determine the complexity factor of the casting which will make the sand 3D printing economically viable. The research analyzed various geometric attributes which can influence the parts' complexity. One of the promising benefits of sand 3D printing is that the mold manufacturing cost remains fairly constant with level of complexity unlike mold making by traditional means. [18]

Durgesh Joshi & Bhallamudi Ravi predicted the complexity factors and find out the method of quantification of various geometric attributes of the cores and mold. It has been observed that the tool manufacturing cost depends on the several factors such as number of cores, volume of part, surface area of the part, core volume, draw distance and variation in section thickness. Below will be presented series of equations with expected set of output values obtained anywhere between 0 and 1. Higher values will represent more part complexity.[27]

- **Part Volume Ratio (C_{PR})**

This ratio is the volume of part to the volume of bounding box, where volume of bounding box is determined using maximum values of length, width and height of the mold. This is defined as,

$$C_{PR} = 1 - \frac{V_P}{V_b} \tag{10}$$

Where Vp is the volume of the part and Vb is the volume of the bounding box. Note that when the volume of part is almost equal to bounding box volume, lower material removal is needed and hence lower machining cost.[18]

- **Area Ratio (C_{AR})**

This ratio is determined by finding the surface area of an equivalent sphere (corresponding to same part volume) to the surface area of the part. Since the sphere has the minimum surface area per unit volume compared to other geometry so this has been kept as reference. This is defined as,

$$C_{AR} = 1 - \frac{A_S}{A_P} \tag{11}$$

Where As is the surface area of the equivalent sphere of same volume while Ap is the area of the part. More surfaces and features in mold geometry will increase the complexity and hence higher machining cost. [18] Equivalent surface area of the sphere can be determined as,

$$A_S = (4\pi)^{1/3}(3V_P)^{2/3} * A_P \tag{12}$$

- **Number of Cores (C_{NC})**

Cores are the hollow sections in the casting which are added so that liquid metal don't fill up the mold completely. Cores are kept based on the design requirements of the part. Cores in the mold can be of different geometry and shapes and thus each core requires separate tooling operation. This factor is defined as,

$$C_{NC} = 1 - \frac{1}{\sqrt{1 + N_C}} \tag{13}$$

Where Nc is the number of cored features. [18]

- **Cores Volume Ratio (C_{CR})**

The greater the core size, the more material will be utilized and greater will be the tooling cost. In this ratio, bounding box volume Vb is used to keep the reference of calculation same. This factor is defined as,

$$C_{CR} = 1 - \frac{\sum V_{Ci}}{V_b} \tag{14}$$

Where Vci is the volume of cores. [18]

- **Thickness Ratio (C_{TR})**

Thickness ratio is the ratio of the minimum to maximum thickness of the part. Thinner section requires more detailing and hence higher tooling cost. This factor is defined as,

$$C_{TR} = 1 - \frac{T_{min}}{T_{max}} \tag{15}$$

Where Tmax and Tmin are the maximum and minimum part thickness respectively. [18]

- **Depth Ratio (C_{DR})**

Depth ratio is defined as ratio of half of the minimum dimension of the part to the draw distance which is the maximum depth of the tooling. This factor is determined as,

$$C_{DR} = 1 - \frac{0.5(min(L, W, H))}{D_d} \tag{16}$$

Where L, W, H are length, width and height of the part respectively and Dd is the draw distance. This ratio shows the part with higher draw distance (higher tooling depth) will have higher complexity. Regression analysis of 40 different industrial parts have been used to determine the relation of the shape complexity of new part, given by the equation below.

$$CF_{estimated} = 5.7 + 10.8C_{PR} + 18C_{AR} + 32.7C_{NC} + 29C_{CR} + 6.9C_{TR} + 0.7C_{DR} \tag{17}$$

This regression based equation is a good approximation of determining the complexity of newer parts.[18]

3.2.4 Prototype Development

Sand 3D printing is a convenient and efficient process delivering the final mold in lesser time and hence can be used to develop prototypes of cores and molds. This is espeicially if multiple design are needed to be made for example with slight changes in part geometry while adding or removing intricate part details.

3.2.5 Environmental Impact and Worker Safety

A good sand mold is essential for quality metal casting, and with growing demands for sustainability, research into alternative molding materials continues. One study done at Aalto University in Finland focused on exploring various sands, binders, and additives, with a particular emphasis on inorganic solid silicate binders due to their environmental advantages. Concerns over VOC emissions from organic binders and increased binder usage in 3D-printed molds highlight the need for eco-friendly alternatives. A series of tests—such as mold strength, gas emission, and 3D scanning—were conducted to assess performance. The findings aim to support a transition from organic to inorganic binders and advance sustainable casting practices, especially in additive manufacturing contexts.[28]

3.3 Filling System Design

Vasková et. al., was able to determine the optimum geometry of the gating system by minimizing pouring time through the use of Magma5 software (MagmaSOFT 5.0). The material used for this study was cast iron EN GJL 250. Fast filling time leads to faster solidification while reduces the shrinkage of the metal, while increasing the yield. The study considered the 5760 different gating system geometries. Magma5 has the ability to internally select the best out of all the geometries based on less filling time. After finding the optimized geometry for gating system, the pouring time was reduced from 15 seconds to to 12 seconds with sprue being completely filled after 4 seconds of pouring. The case study considered the DISAmatic molding line at Zleivearen SEZ Krompachy. The maximum performace is 330 molds/hour. With the original pouring time of 15 seconds, 400 casting pieces were obtained in one hour which increased to 480 pieces/hour with 12 seconds pouring time thus increasing the yield by 20%. These results were practically applied at the molding line and results showed good quality castings with improved yield. [29]

A research conducted at Daido University in Japan by Kosuke Taki et. al studied the flow of molten aluminum alloy through casting filter installed at sprue. This is done in order to reduce the molten metal velocity and to make the metal flow laminar to reduce the air-entrapment. [30]

One study conducted by Pennsylvania State University and Hazleton Casting Company from US used computational flow simulations to study the effectiveness of 3D Sand Printed (3DSP) molds in metal casting. Three different sprue designs were considered, straight, parabolic and helical-conical. Molds were only made for helical-conical sprue design. The mold design was done with horizontal and vertical parting lines to compare different results of the study. CFD simulations and CT scan of the melt flow in mold show that helical-conical casting reduced the defect volume by 99.5% when compared to straight sprue casting. Furthermore, reduced inclusions in part lead to significantly higher flexural strength compared to straight sprue casting. The CT scans showed the void size of $3mm^3$ in case of helical conical sprue design while being 608 mm3 and 269 mm3 for straight and parabolic designs. [31] The Figure 3 shows these designs.

Figure 3 Different Sprue designs attached to offset basin. Helical Sprue reduce the melt velocity most. Picture: Santosh Reddy et.al.

K. Munpakdee et. al., studied the effect of sprue size on porosity defects in Platinum 950 alloy made for jewellery applications using computational approach. The research utilized the FlowCAST 3D software for this purpose. Two spure sizes were taken consideration and expereimental results were noted using image analysis. It was found that the bigger feed sprue size led to lesser porosity compared to smaller sprue size. [32]

A number of studies have found reduction in casting defects and improvement in casting accuracy through the utilization of multiple spures instead of single sprue. One study from Brazil studied the effects of single and double sprue designs on the accuracy of Nickel-Chromium crown casts developed for dentistry applications. The goal was to determine and compare the crown margin accuracy from both designs. A total of 88 models sprue models were studied, 44 of each sprue design. A marginal discrepancy was observed with a mean of 43.1 ±

4.74 µm was observed in case of single sprueing system while for double sprueing system a mean of 25.7 ± 4.25 µm was found. This difference is statistically significant ($p<0.05$). It was concluded that double sprue designs developed more accurate margins than single sprue design. [33]. A number of other studies also had similar results. [34–37]

A research conducted at King Saud University in Saudi Arabia investigated the effects of gating system design on the mechanical properties of 6063-T5 Aluminium alloy in sand casting process. Bottom and top gating configurations were considered for filling the mold cavity. Three input parameters including pouring temperature, runner area and ingate area were noted. A series of experiments were performed using Response Surface Methodology (RSM) and bottom filling system was found to be better configuration. The specimen developed using this approach displayed 4.08% - 18.78% higher ultimate tensile strength (UTS) and 5.98% - 20.60% higher percentage elongation. [38]

The effect of filters types on mechanical properties were noted in one of the research conducted at Univeristy of Zilina, Slovakia for aluminium alloy casting. Porosity, tensile strength, yield strength and percentage elongation were noted as the mechanical properties for experiments. The goal of the study was to minimize the reoxidation process by reducing the melt flow velocity using different filters such as labyrinth filters, foam filters and flat filters. The labyrinth filters were shown to be the best in reducing the melt flow velocity but didn't gave the better mechanical properties. The best overall properties were achieved in case of foam filters. [39]

3.4 Effect of Gating Design on Flow Characteristics

Gating ratio is one of the important aspects to take into consideration when designing the gating system. One study performed casting of Al-Si alloyed plates of various thickness using non-pressurized gating with 1:4:4 gating ratio and green sand moulding technique. The plate castings were visually inspected for surface defects and X-ray radiography was used to check the internal defects and it was found that the casting had no defects and quality castings were produced. [40]

One study determined the effect of multi-gating system in casting through simulation and simple experimental based model. The experiment was carried out using a water model. Four different filling system configurations were taken into consideration. Two of them had a straight runner and other two had tapered runner. The sprue placement was kept at two different

locations. The first sprue placement at the starting end of the runner will all 4 ingates to one side. The second sprue placement was in the middle of the runner with 2 ingates on each side. It was found that tapered cross-section with centered sprue placement is optimum for having a balanced flow rate and less filling time. [41]

A research presented a comparative analysis of different gating systems using computer simulations carried out on Novacast and Magmasoft for steel castings. It was found that computer simulations can effectively predict the velocity and turbulence characteristics of flow but fail to determine the bubble formation in flow. It was found that naturally pressured filling system was effective in reducing the formation of entrainment defects, while the vortex filling system and refractory tube based system performed poorly. Naturally pressurized system, filling system with runner and large spin trap at the end of runners were proven to be great for reducing flow velocity. [42]

The goal of one study was to maximize the filling rate of metal into the mold as this can improve the access of metal to thinner sections, improve the yield and reduce the chances of cold shuts and misruns. Pouring time, modulus of ingate, mold erosion, Reynolds number and quick filling were the possible constraints for filling the mold quickly in sand castings. To optimize the filling rate of melt into the mold cavity, Sequential Quantitative Programming (SQP) was used for this task. [43]

3.5 Slag Formation and Gating System

Slags are formed in the liquid metal as a result of oxidation of certain elements in the melt like Al, Si, Mg etc. Also the slag can be formed as a result of deliberate addition of these elements. The major problem arises if the mold cavity has some water vapour or oxidation elements inside which can cause the formation of slag inside the mold. The problem also arises as a result of filling system pushing the melt at turbulence speeds causing a lot of air to pass through the melt and this can cause oxidation leading to formation of slag. Runners can be designed specifically to skim of the excess slag. Most of the slag is formed at the entering meniscus of the flow and this can be skimmed off by extending the runner after the ingates and making a dead end. This is referred as dead runner. This makes sure that excess slag is contained in the dead end and clean melt enters the mold. Furthermore, similar results can be achieved using saw-tooth runner. [44]

Shuvo et. al., investigated the role of vortex chambers in slag trapping for ferrous metals through computational and experimental analysis. 6 different designs of vortex chambers were compared with the benchmark straight runner section. It was found that for one of the designs of vortex chambers the melt velocity reduction was 31% at the ingate confirming the reduction in turbulence and re oxidation in melt stream. This directly co-related with less slag formation in the process. [45]

Slag formation can cause major problems in slab casting and thus needs to be addressed. One study conducted by Wang et. al., found some promising results. Optimization study was performed on reducing slag entrapment in 1270 x 150mm slab by continuous casting. The effect of Submerged Entrance (SEN) Depth and casting speed was studied using computational software. The results showed the optimum properties were achieved at SEN depth of 90 mm and casting speed of 1.6 m/min. Under these conditions, maximum surface velocity was smallest at 0.335 m/s and maximum slag entrapment ratio to be 0.44% at a depth of 0.1m below the meniscus after 15 seconds. The results were confirmed later by water modelling. [46]

Some of the research is being directed towards the development of model to predict the amount and location of oxides in castings. Mean diameter of these oxides are taken into account when making the model. Parameters like density, drag and wall friction effect the motion and location of oxides. A lot of casting inlet parameters are taken into account when prediciting the location and amount of these oxides and have good agreement between measured and simulated results. [46, 47]

Recent studies have highlighted that in aluminum alloy castings, mechanical properties are often more significantly influenced by entrained defects, particularly bifilms, than by microstructure alone. To evaluate their impact, the Reduced Pressure Test (RPT) has been employed as an effective method for quantifying bifilm content in terms of their length and frequency. The resulting bifilm index has emerged as a sensitive indicator of melt quality, correlating strongly with the number of pores observed. Research shows that both bifilm index and pore count can jointly assess metal quality, and the near absence of bifilms is associated with remarkably high ductility in cast aluminum alloys. These findings reinforce the importance of bifilm control in improving casting performance. [49]

4 Research Methods

4.1 Materials and Material Data

Aluminium alloy (AlSiMg10) is used to study the effect of gating system on mold filling. Table 1 shows the detail of material properties related to AlSi10Mg alloy.

Table 1 Material Properties for AlSi10Mg alloy used for Flow3dCast Simulation

Property	Value	Notes
Alloy Name	AlSi10Mg	Aluminum-Silicon-Magnesium alloy
Silicon Content	~10 wt%	Improves castability and fluidity
Magnesium Content	~0.3–0.5 wt%	For precipitation hardening
Density	2.65–2.68 g/cm³	
Melting Range	570–595 °C	Eutectic melting range
Casting Temperature	710–740 °C	Pouring temperature
Solidification Shrinkage	~0.6–0.8%	Important for riser design
Thermal Conductivity	~130–150 W/m·K	High; good for heat dissipation
Thermal Expansion Coefficient	~21–23 ×10⁻⁶ /K	Affects dimensional changes
Tensile Strength (as-cast)	~200 MPa	Increases with heat treatment
Yield Strength (as-cast)	~110 MPa	
Elongation (as-cast)	~2–4%	Brittle in as-cast condition
Hardness (as-cast)	~65–75 HB	Increases after aging
Modulus of Elasticity	~70 GPa	
Fluidity	High	Excellent for thin-wall castings
Corrosion Resistance	Good	Especially in marine environments
Machinability	Good	
Heat Treatment	T6 (solution + aging)	Improves strength and hardness

AlSi10Mg has excellent strength to weight ratio and provides superior strength properties at high temperatures. In general, the material has good workability and weldability, thus making it a great choice for automotive and aerospace applications. Furthermore, the material has good fatigue strength and good heat crack resistance.

4.2 Casting Methods and Mold Designs

4.2.1 Design with single ingate:

The mold design consisted of numerous calculation to get to the best mold design possible. Several adjustments were made in the later stage to limit the velocity of the flow. The sprue is designed to handle metal mass of approximately 0.5-0.7 kg. The mold cavity is assumed in the form of a block to note the effects of solidification with needed accuracy. The mold cavity dimensions are 40mm x 20mm x 100mm. The metal enters the mold from the longer side. Bottom feeding of metal is taken as it is the best configuration to fill the mold. This is done to avoid turbulence and bubble entrainment. The Figure 4 below shows the model of the cast geometry developed using Solidworks. The model is for single gate design. The surrounding grey block is hidden in the image is the mold block used in gravity sand casting. The red and green balls shown in the image below represent the openings of pouring basin and feeder to air and they are kept as air vents in the design. The disc shape in the pouring basin represents the metal inlet.

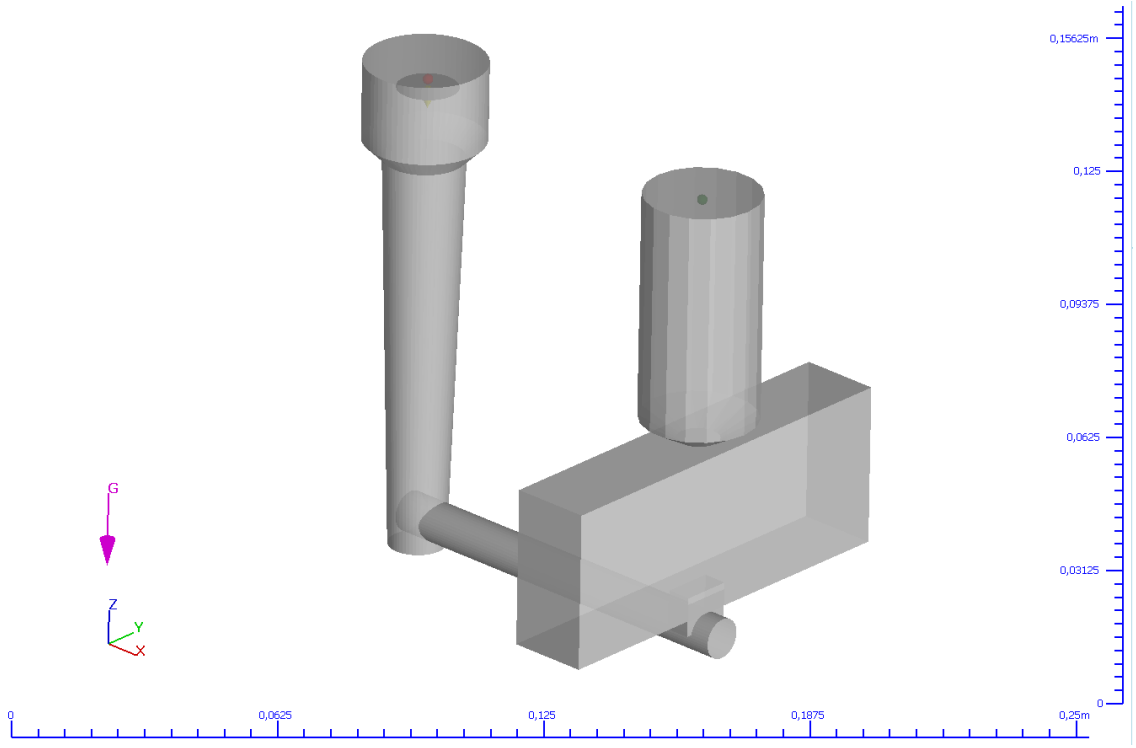

Figure 4 Filling System with Single Ingate Picture: Umar Siddique

The various dimensions of the filling system is shown by the table below.

Table 2 Filling System Dimensions

Parameters	Dimensions
Pouring Basin Diameter	30 mm
Pouring Basin Depth	30 mm
Sprue Entrance Diameter	20 mm
Sprue Height	125 mm
Sprue Exit Diameter	13.5 mm
Runner Diameter	10 mm
Runner Length	100 mm
Ingate Dimensions	8mm x 12mm x 15mm
Mold Cavity Dimensions	40mm x 20mm x 100mm
Feeder Dimensions	R29 mm; H58 mm

The runner length was divided into 4 imaginary sections of 25 mm each and the useful of this would be evident in next designs as it would help us to keep the flow length same through all sections. The second important consideration to make here is that feeder dimensions are taken by reference values from literature [50]. The formula for determining the volume of feeder derived from casting handbook from Campbell [3].

$$V_f = \frac{\alpha}{e - \alpha} V_c \tag{18}$$

Where,

α: Solidification Rate; for Aluminium alloys 7% (0.07)

e: Feeder Efficiency; for cylindrical feeders with H/D=2: 18% (0.18)

V_c: Volume of Casting

V_f:Volume of Feeder

Feeder neck is a tapered section at the base that aids the appropriate filling of the metal and also makes it convenient to feed the metal during solidification phase. This can observed from the image above.

4.2.2 Design with 2 Ingates:

The second mold design has two ingates at the end of the runner. Both end points of runner have the same travel length from the sprue exit. This is important to make sure that flow is equally branched out through both ingates equally. The Figure 5 below shows the bottom view of the mold. Bottom feeding has been used to avoid the free-fall of metal and to restrain the velocity of liquid melt.

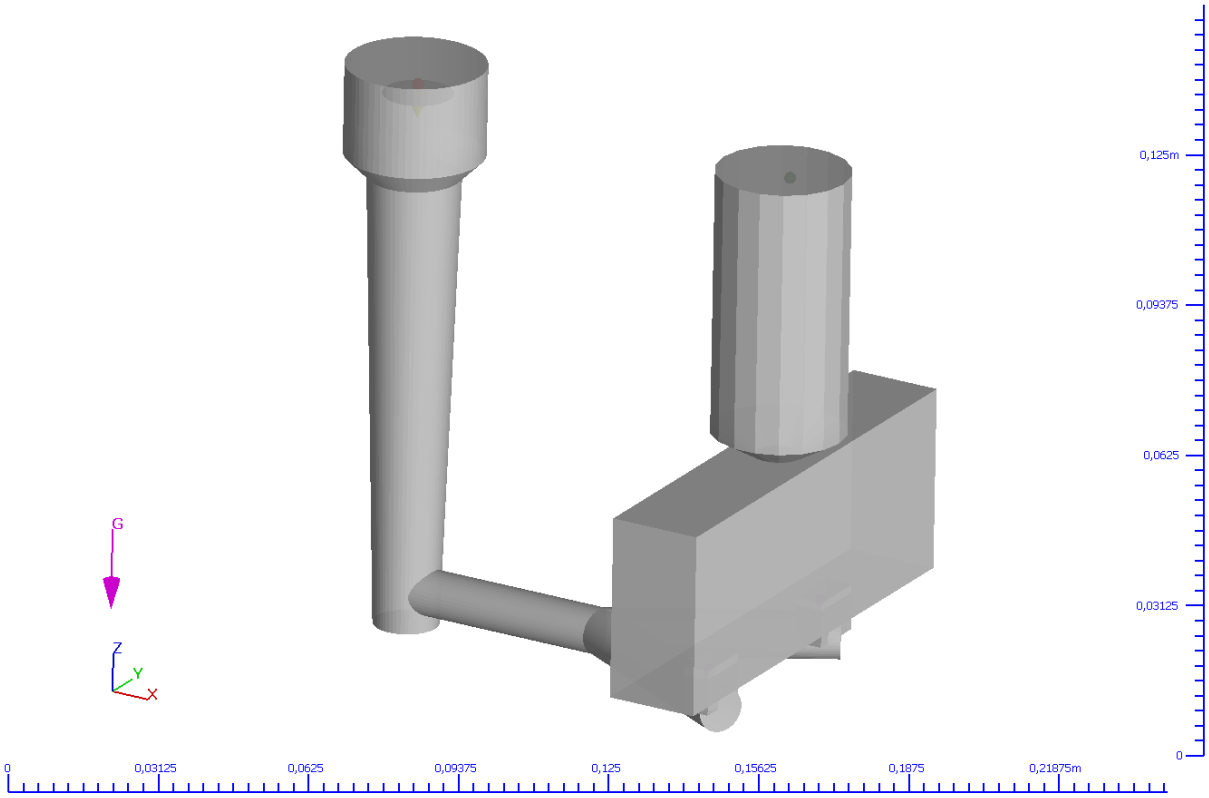

Figure 5 Filling System with 2 Ingates Picture: Umar Siddique

4.2.3 Design with 4 Ingates:

Increasing the number of ingates allows the faster pouring of the metal into the mold and thus should theoretically lead to reduction in filling time. The Figure 6 below shows the isometric view of the filling system with 4 ingates. All four ingates are aligned along the direction of flat longer side of the mold cavity to visualize the melt flow better.

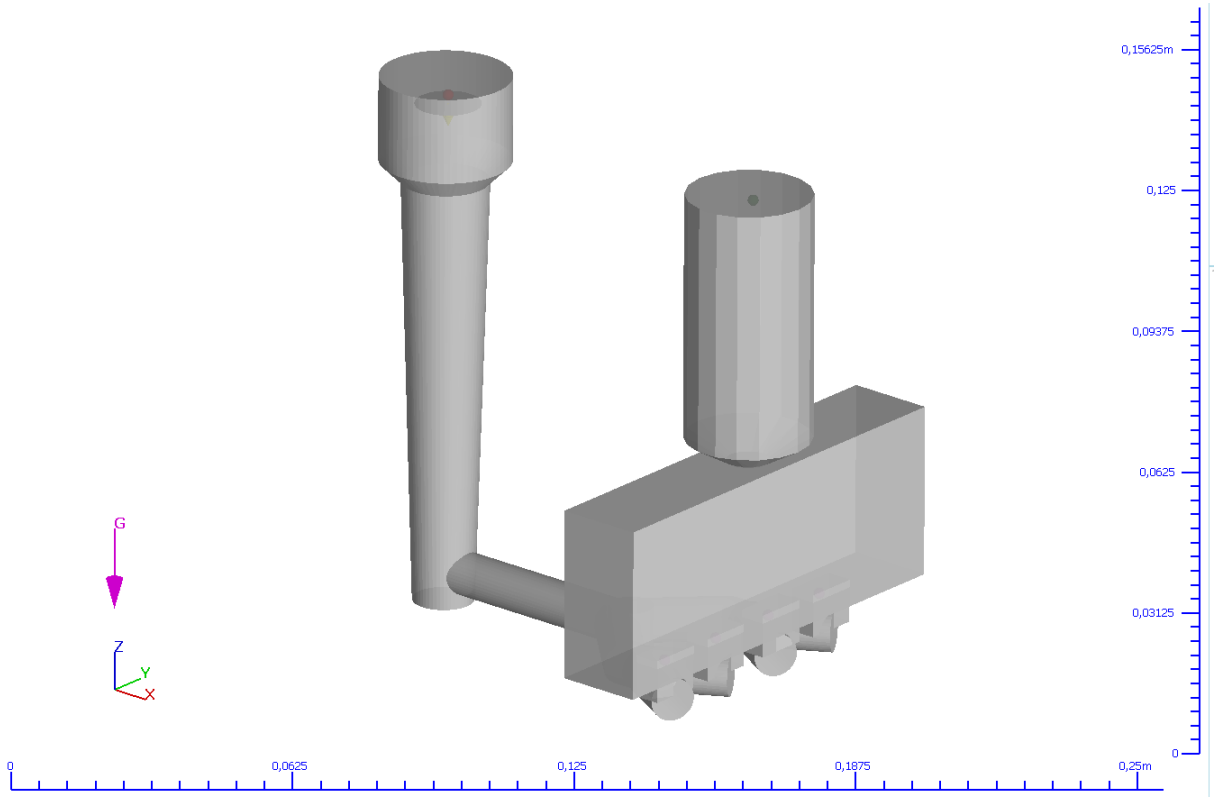

Figure 6 Filling System with 4 Ingates Picture: Umar Siddique

The Figure 7 below shows the bottom view of the 4 ingates filling system. This view is specifically provided to note the lengths of various sections of runner. Total runner length is 100 mm which is divided into 4 regions of 25 mm length each. It can be noted from the image below that first 2 regions are straight while 3rd and 4th regions are made to divide the flow into branches. This is done to restrict the flow speed under the critical limit of 0.5 m/s. Dividing the runner into fixed length regions allowed to keep the travel distance from ingate to sprue exit same for all the gates. Further it helped greatly with setting up the flow rate of metal at the inlet by giving a good approximation of total runner volume.

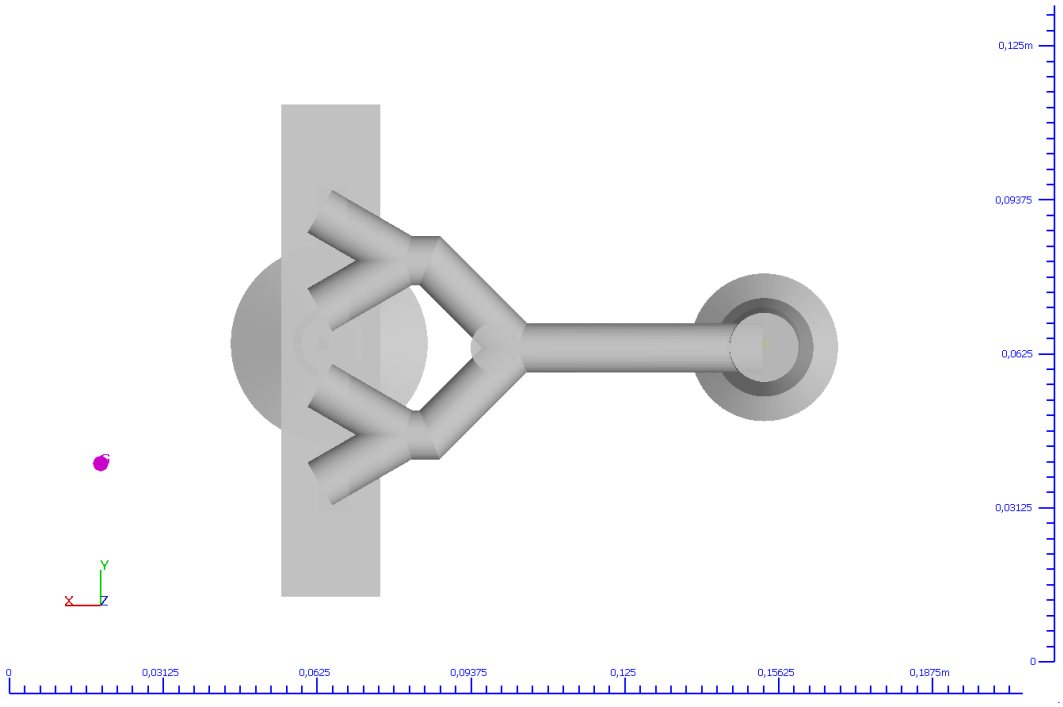

Figure 7 Filling System with 4 Ingates (Bottom View) Picture: Umar Siddique

4.2.4 Design with 4 Ingates and Alternate Filling (Test Case):

An alternative design is proposed with an offset basin and slightly narrower sprue than previous model. This sprue size was determined using the Bernoulli's law and slightly adjusted to make the melt flow conveniently through the sprue. Sprue has a curved end as can be seen from the Figure 8 below.

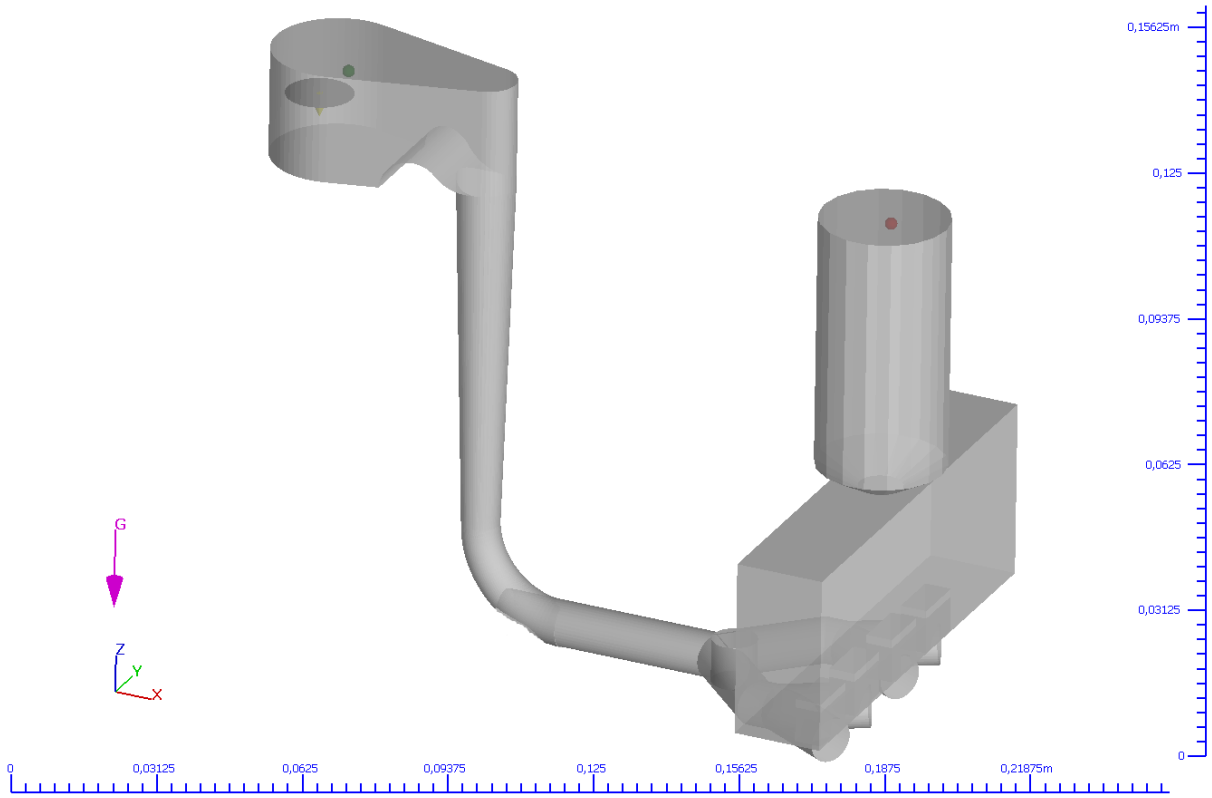

Figure 8 Alternate Filling System with Offset Basin and Curved Sprue Exit. Picture: Umar Siddique

The dimensions of this sprue are:

Sprue Inlet Diameter: 10 mm

Sprue Outlet Diameter: 6 mm

Sprue Length: 125 mm

4.3 Computational Models

The basic 3D model of mold was made using Solidworks. The gating system design was designed such that to achieve the entrance velocity of 0.5 m/s as described by Campbell to be an optimum velocity for aluminium alloys. The computation model is made for 1 gate, 2 gates and 4 gates filling system to determine the effect of gating ratio on the filling properties. After a number of design iterations it was found that the gating ratio of approximately 1:1:1.7 is most suitable in our case. The computational simulation is to be performed in a series of steps. In the first step, filling simulation with single gate is performed. The second and third steps deal with filling simulation for 2 and 4 gates filling system. The fourth step is to improve the 4 gates filling system design and in the last step filling and solidification simulation was done for the

improved 4 gated filling system. Computational simulation was performed based on the model setup done using FlowCAST 3D.

4.3.1 Courant–Friedrichs–Lewy (CFL) Condition

The numerical model of the software is based on certain convergence criteria referred as, Courant–Friedrichs–Lewy (CFL) Condition. This is the primary condition for numerical stability in transient flow simulations:

$$\Delta t \leq \frac{\Delta x}{v} \tag{19}$$

Where:

Δt = time step

Δx = grid cell size

v = local flow velocity

CFL condition is used to model the advection phenomenon and this condition is applied for finite difference approximation of partial differential equations. This ensures that flow does not move more than one mesh grid cell in a single time step, preserving numerical stability in fluid dynamics. The continuous flow model equation for 1-D case is,

$$\frac{\partial w}{\partial t} + u\frac{\partial w}{\partial x} = 0 \tag{20}$$

CFL condition has the following form,

$$C = \frac{u\Delta t}{\Delta x} \leq C_{max} \tag{21}$$

Where,

C; Dimensionless number referred as Courant number

u; Magnitude of velocity

Δt; Time step

Δx; Length interval

4.3.2 Re-Normalization Group (RNG) Viscosity Model:

This model is used by FlowCast 3D to account for viscosity effects in flow. The model is similar to k-epsilon model except it introduces additional term in its epsilon equation which increases accuracy for the strained flows. Also the model takes into account the swirl effect on turbulence enhancing accuracy. Unlike the standard k-epsilon, RNG model accurately depicts low Reynold's number flow based on analytical relations for determining effective viscosity.

4.3.3 Model Setup for FlowCAST 3D

Some of the key default model setup conditions were set as follows. These conditions were kept same while simulating all the mold design cases.

- Materials: G-AlSi10Mg (Metal); Air (Gas)
- Geometry: Sand Mold set as Remaining Space; filling components (sprue, runner, feeder, ingate) set as Cavity; Cuboid (40mm x 20mm x 100mm) set as Casting Part.
- Mesh: Flow Mesh; Size of cells = 0.002 m
- Boundary Conditions: Symmetric on all faces except top face (Z Max) taken as Pressure.
- Heat Transfer conditions: Metal to Void = 30 $W/m^2/C$; Metal to Sand Mold = 1000 $W/m^2/C$ (Liquid Metal); Metal to Sand Mold = 400 $W/m^2/C$ (Solidified Metal); Sand Mold to Void = 30 $W/m^2/C$
- Vent: size = 1e-05m; Outlet of feeder
- Output: Interval time = 0.04 s; Output Properties: Entrained air; Fluid fraction; Fluid velocities; Pressure; Surface defect concentration; Temperature of fluid

Under the models tab in solidification section, shrinkage with flow effects was kept off for filling simulation. The simulation is to be performed by viscous flow assumption and viscosity was determined using RNG (Re-Normalization Group) model which is a type of k-epsilon turbulence model.

Following are the two simulation variables that were changed for each design. It is to be noted that as the number of gates increased, so does the effective area of the ingates. To keep the velocity constant at the gates, theoretically it was possible to increase the input flow rate proportionately since the effective gate area increased with higher number of gates.

- Time Controls:

  Finish Time = 7s with 1 ingate

  Finish Time = 4.7 s with 2 ingates

  Finish Time = 3.5 s with 4 ingates

  Fill Fraction = 0.999 (Additional finish conditions)

- Metal Input: From pouring basin top inlet; Inlet Diameter = 0.015 m; Metal Temperature = 720 C;

  Flow rate = 2.5e-05 m^3/s with 1 ingate

  Flow rate = 3.75e-05 m^3/s with 2 ingates

  Flow rate= 5e-05 m^3/s with 4 ingates

The Figure 9 below shows the plot of filling rate with time for 3 different gating designs presented in this paper. As we know that the total volume is equal to volume flow rate multiplied by the time it takes to fill that volume (given by total area under the curve), this means that

With Single Ingate; (2.5e-05 m^3/s)*(7 s) = 17.5e-05 m^3

With 2 Ingates; (3.75e-05 m^3/s)*(4.67 s) = 17.5e-05 m^3

With 4 Ingates; (5e-05 m^3/s)*(3.5 s) = 17.5e-05 m^3

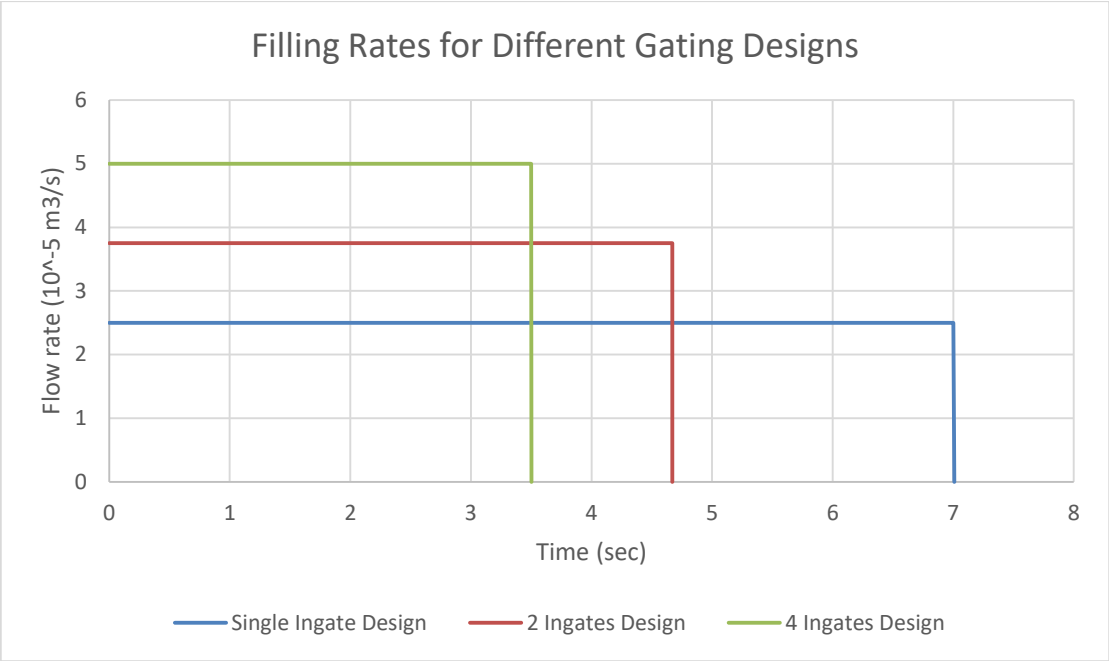

Figure 9 Plot showing different input metal filling rates used for different gating designs. Picture: Umar Siddique

The test case with alternate filling system is kept as separate with separate filling conditions. Test case was added to check if it is appropriate to increase the flow rate even more as this could reduce the filling time. To check the results, following flow conditions were used.

Finish Time = 3 s with 4 ingates and alternate filling

Flow rate = 6e-05 m^3/s with 4 ingates and alternate filling

5 Results and Discussions

This section entails the simulation results explaining the velocity at ingates. Contour maps are provided at specific intervals along with plots of average velocity with time. Further it sheds some light on air entrapment in case of 4 ingates and suggestions to improve the filling system.

5.1 Simulation Results

5.1.1 Velocity Analysis with Single Ingate

The Figure 10 below shows the initial pouring of melt into the pouring basin. It can be seen that flow entered at a velocity of approximately 1 m/s and due to free fall it sped up to approximately 1.2 m/s. As the melt falls into the sprue well, the flow stops and starts filling the well. This did a great job in restricting the flow speed. The flow in the runner is made possible due to the height of the melt in the spure well, which created sufficient head pressure for the melt to flow out.

Figure 10 Side View showing filling at time 0.32 sec Picture: Umar Siddique

The speed of the melt in the runner is directly proportional to the level of fluid in the well based on hydrostatic law defined by Toricelli's law as,

$$v = \sqrt{2gh} \tag{22}$$

Where h is the height of the fluid in the sprue well and g is the gravitational constant. This law is an approximation as it assumes the fact that the level of fluid in spure well changes negligibly with outlet flow which is not true in this case. However the law gives an understanding of the relation between outlet velocity and level of fluid.

The Figure 11 below shows the gate view of the mold. The snippet is captured at the point of approach of the melt flow at the mold cavity inlet. Theoretically, the flow is at highest speed at the initial approach, since there is no weight of the overhead metal. From the contour map, the flow is approaching close to 0.5 m/s.

Figure 11 Gate View showing filling at time 0.48 sec Picture: Umar Siddique

The Figure 12 below shows the behavior of the liquid melt as it enters the mold cavity. It can be noted that the speed of the melt is under the critical limit of 0.5 m/s. Due to this melt is not

jetting into the cavity and smoothly spreading onto the mold base. This is done to ensure that minimum air is trapped in the melt as it could lead to major defects in solidified part.

Figure 12 Gate View showing filling at time 0.68 sec Picture: Umar Siddique

The Figure 13 shows the plot of average ingate velocity with time. The data points were taken from the Flow3D-Post. The ingate velocity was determined at each of the time steps of size 0.04 sec by the software. The data points were then plotted using MS-Excel. It can be seen that more varying speed at the inlet gate can be observed at the earlier stages of filling. This is due to the metal in the mold spreading from the point of entry. As the melt flow spreads out from the ingate section into the mold cavity, the incoming metal rushes in creating a peak or a crest. As a result of sloshing effect, the metal bounces back of the mold cavity walls, thus covering the ingate which hinders the flow of incoming metal and thus reducing its speed, giving a valley or a trough. Further variations in inlet velocity are subject to sprue well filling affecting the flow of melt in runner. As the level of the fluid in the cavity rises, the sloshing effect of melt reduces and thus the plot curve has become relatively smooth towards the end.

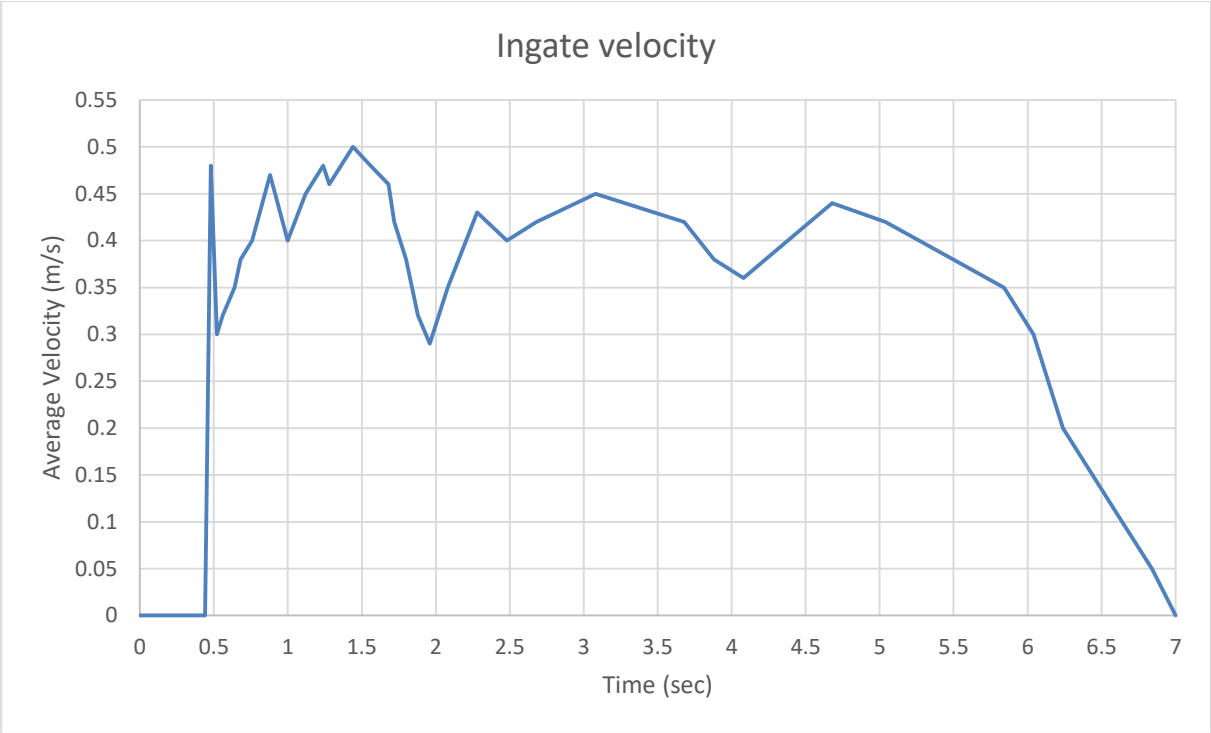

Figure 13 Plot of average ingate velocity with time for single ingate design Picture: Umar Siddique

5.1.2 Velocity Analysis with 2 Ingates

The Figure 14 below shows the velocity of the melt passing through the runner section for 2 ingates filling system. In this case the melt is entering the sprue at a higher flow rate of 3.75e-05 m^3/s. Just as for single ingate, the sprue well fills up immediately and provide the excess flow to runner. The flow then speeds up in the runner section to approximately 0.6 m/s. The sprue well also tends to reduce the turbulence of the flow, by reducing the free fall speed. As the flow passes through the runner and passes through the 2 ingates the velocity at gates remain same, even though the flow rate is increased. This is due to the continuity equation.

$$A_1 v_1 = A_2 v_2 \tag{23}$$

The basic assumption of this equation is that the flow is continuous and doesn't break, which is true for runner section in this case.

Figure 14 Side View showing filling at time 0.32 sec for 2 ingates design Picture: Umar Siddique

The Figure 15 below shows the gate view. It can be observed that liquid melt approached the ingates below the critical limit of 0.5 m/s. The light blue lining can be seen near the entry section to mold cavity showing the speed of entry at about 0.5 m/s.

Figure 15 Gate View showing filling at time 0.48 sec for 2 ingates design Picture: Umar Siddique

The Figure 16 below shows the smooth entry of the flow into the mold cavity without any jetting effects. Further it can be seen that the flow is contained and spreading uniformly along the base of the mold cavity.

Figure 16 Gate View showing filling at time 0.68 sec for 2 ingates design Picture: Umar Siddique

The Figure 17 below shows the plot of the average velocity at 2 ingates of gating design. It can be noted that in this case the initial peak velocity as the melt approaches the ingate is not the absolute maximum velocity. This is because the melt flow was not fully developed inside the mold cavity. After the initial peak, sudden dip can be observed which is due to fact that melt in the mold cavity is having sloshing effect and hindering the inlet flow. But as the flow is developed to a certain level inside the mold cavity and the sloshing effects diminished the inlet velocity at both gates increased gradually reaching a maximum of around 0.4 m/s at around 1.5 seconds time. While comparing the two gates the velocity at gate 1 is slightly higher at most time steps than velocity at gate 2, though the runner system is symmetrical. These minor differences is due to flow discontinuities at some point in flow which can cause melt to direct

in one direction slightly more. Furthermore, more peaks can be observed at the earlier portion of the plot which shows erratic flow behavior during the approach of melt.

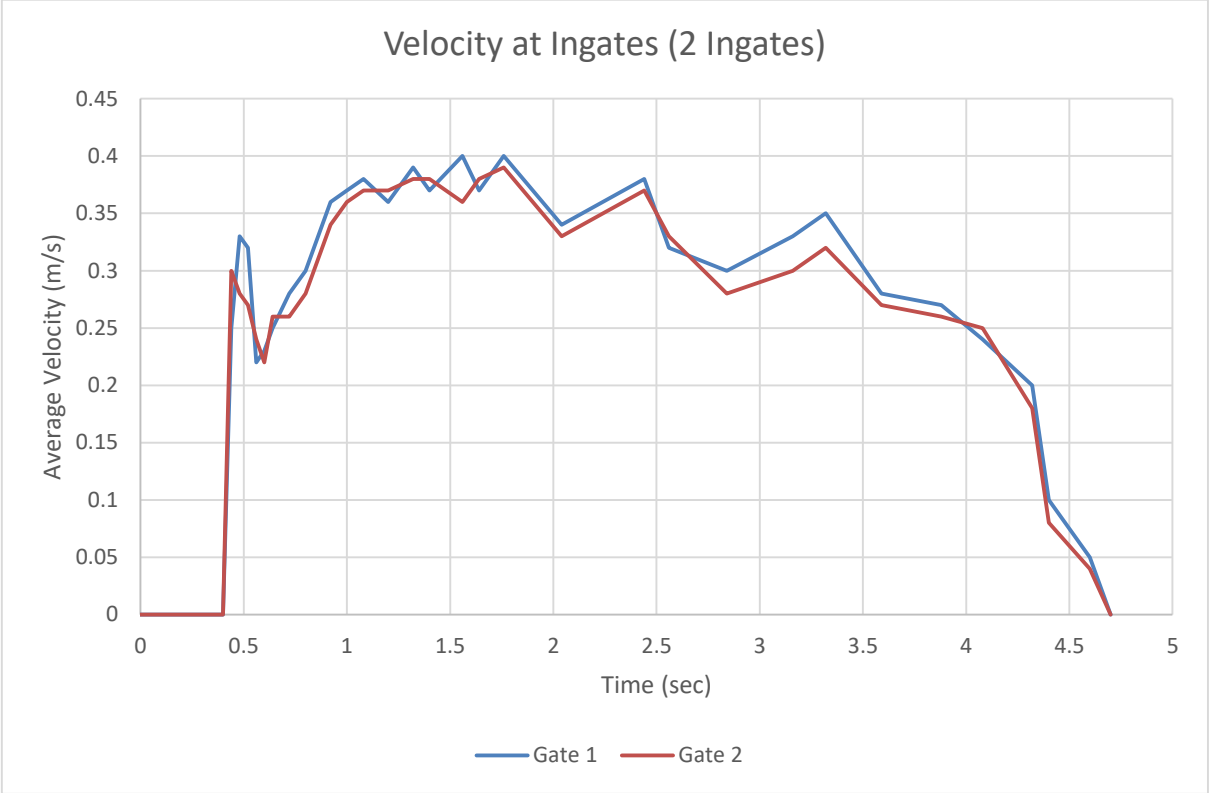

Figure 17 Plot showing average velocity with time at 2 ingates Picture: Umar Siddique

5.1.3 Velocity Analysis with 4 Ingates

The increasing flow rate of melt demands increasing the area to keep the velocity at the gates constant. This is done by increasing the number of gates thus increasing the effective area of the flow. The Figure 18 below shows the entry of melt into the 4 ingates filling system. The flow enters at a speed of approximately 0.8 m/s from the sprue inlet. Due to the free-fall the flow gains considerable speed of 1.2 m/s. As the melt reaches the spure well, the flow stops and starts filling the well before it was able to flow out through the runner. The flow then accelerates in the runner section and after that it faces restriction as it passes through the first branch and then the velocity drops even further as it passes through the second branch before entering the mold cavity.

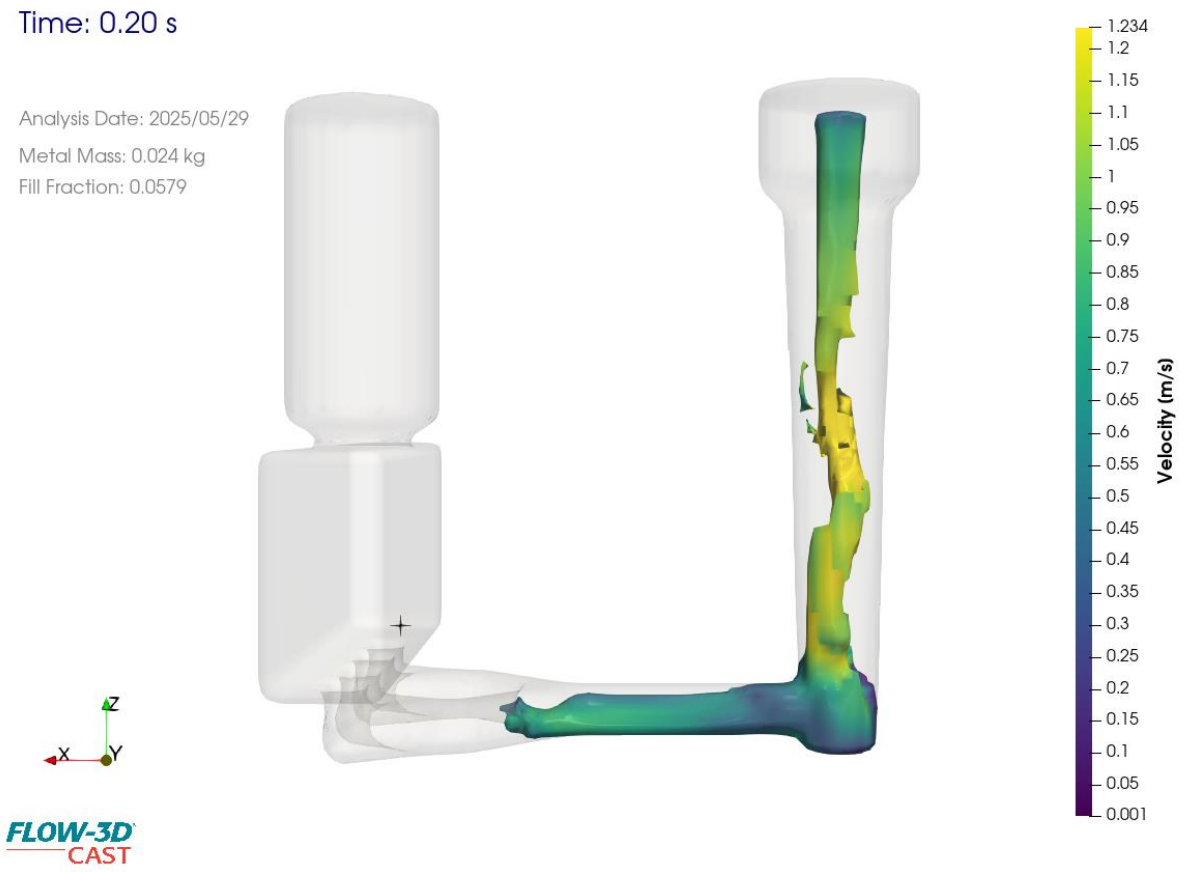

Figure 18 Side View showing filling at time 0.20 sec for 4 ingates design Picture: Umar Siddique

The Figure 19 below shows the gate view as the melt approaches the 4 ingates. The gates are labelled are in this case for convenient identification. It can be seen that fluctuations in flow is evident in this case. The flow from ingate 3 is retarded and is taking slightly more time to reach the mold cavity, even though the runner system is symmetrical. This is due to the internal flow discontinuities due to which the flow preferentially moves in one direction more than other. The flow from one gates 1 and 2 has already started to spread out on the base of mold cavity and merging together. This early stage of filling is critical, as improper synchronization between the gates can cause air entrapment or cold shuts. The asymmetry observed in flow behavior highlights the sensitivity of the gating layout to internal resistance and path length. Gate 3, in particular, shows delayed filling, possibly due to slight differences in runner geometry or local turbulence. The interaction zones where different flow fronts meet can also become sites of potential defect formation if not properly vented. Continuous monitoring of such behavior helps in refining the gating system for more uniform and directional flow. This behavior also reflects the influence of dynamic pressure differences within the runner system, which can alter the sequence in which gates are activated.

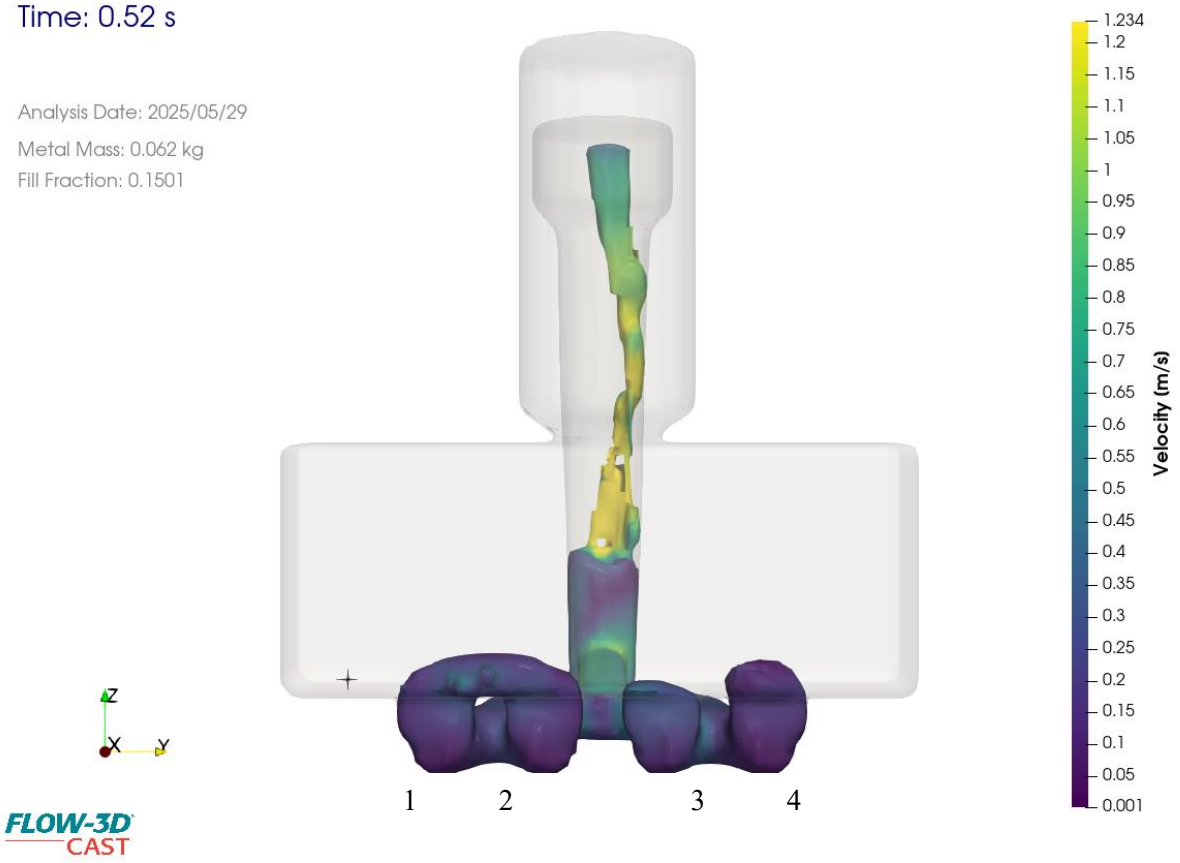

Figure 19 Gate View showing filling at time 0.52 sec for 4 ingates design Picture: Umar Siddique

The Figure 20 below shows the filling at timestep of 0.80 sec. The flow has started to develop and is spreading towards the wall of the mold cavity. An important consideration to make is that velocity at the two extreme gates namely gate 1 and 4 is highest while 2 and 3 is relatively slow. This is because of the smooth transition of the runner sections connecting these gates. This can be also seen from the bottom view of 4 ingates filling system from previous chapter. Due to the layout of the runner, the melt follows the path of least resistance resulting in higher velocities at gate 1 and 4. This is because upon bifurcation, the melt flow directed towards central gates (2 and 3) face more sudden flow changes and obstruction resulting in lower velocity at these ingates compared to gates at extreme ends (1 and 4). It can be seen that velocities at extreme gates is approximately 0.4-0.5 m/s while at central gates around 0.2-0.3 m/s.

Figure 20 Gate View showing filling at time 0.80 sec for 4 ingates design Picture: Umar Siddique

The Figure 21 below shows the plot of the average velocity at the 4 ingates. At a first glance, significant variations can be observed in the flow entering through the ingates. The velocities at gates 1 and 4 are higher than the central gates due to the aforementioned reasons. An initial peak can be seen in the plot showing high velocity of the incoming flow due to no overhead metal in mold cavity. As the melt enters the mold cavity and starts to spread at the base of mold cavity, melt from other ingates start spreading as well and as a result of this interaction a sloshing effect is generated, and this is evident from the initial portion of plot showing high velocity fluctuations in the form of sharp crests and troughs. As the level of melt in the cavity rises the slosh effect diminishes and flow gradually becomes a bit stable. There are a number of fluctuations in the flow, it can be noted from the plot for ingates 2 and 3 at time step of 1.5 seconds, the flow direction changed preferentially towards ingate 3 while flow velocity at ingate 2 is reduced. This might be due to the flow discontinuities happening in the runner section due to sharp bends and flow diversions, causing the flow to suddenly move preferentially in one direction. The filling stops at 3.5 seconds and time step and flow through ingates stop.

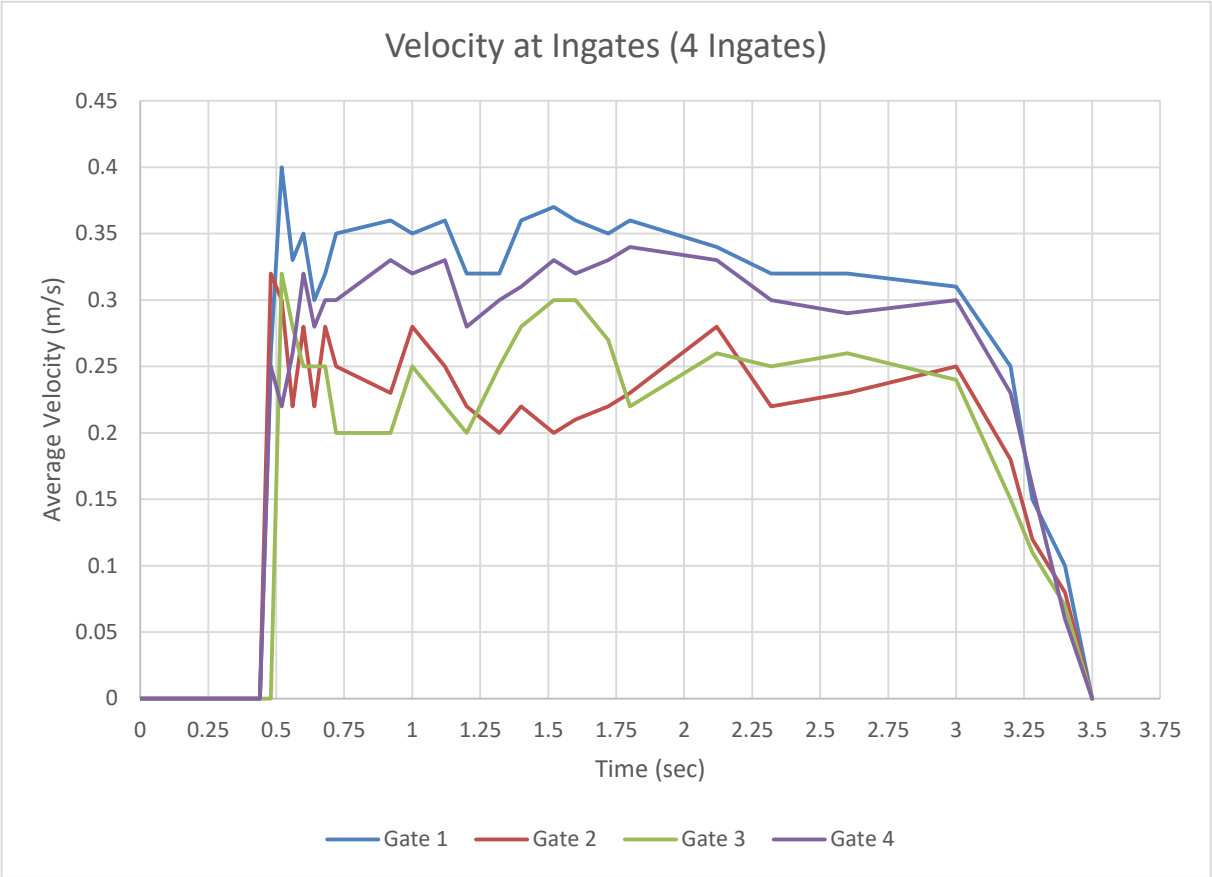

Figure 21 Plot showing the average ingate velocity with time for 4 ingates Picture: Umar Siddique

5.1.4 Velocity Analysis with 4 Ingates and Alternate Filling (Test Case)

The test case simulation was performed with alternate filling system as can be from the Figure 22 below. An offset pouring basin coupled with narrow sprue and curved transition to runner is added. Note that this mold design doesn't include the sprue well as present in previous models. The melt is poured into the deeper section of the pouring basin and fills it up. As the basin fills up, it overflows and passes through the curved wedge and goes smoothly into the sprue. The flow gets developed on a very early stage in the sprue, but at the expense of higher speed. This high speed flow at around 0.8 m/s, then speeds up even more after passing through the narrow end of the sprue and passing through the curved sprue exit. The flow gets a maximum velocity at the start of the runner section of around 1.024 m/s approximately 2 times more than the critical speed at gate. Further it can be noted that as the melt enters the runner, it isn't fully in

contact with runner walls thus possibly leaving air gaps and eventually leading to flow turbulence.

Figure 22 Side View showing filling at time 0.40 sec for 4 ingates design with alternate filling Picture: Umar Siddique

The Figure 23 below shows the initial approach of the melt flow at the gates. The flow appears to be in good condition with speed close to 0.5 m/s and the melt is not jetting. Further the melt is spreading uniformly in all directions.

Figure 23 Gate View showing filling at time 0.60 sec for 4 ingates design with alternate filling Picture: Umar Siddique

The Figure 24 below shows the filling at timestep of 1.0 second. There is one serious problem that must be noted here, as seen from the image, the flow is not fully developed through gate 3 and this caused the average velocity to drop across the gate 3 significantly. Furthermore, this caused the overall melt flow to enter the mold cavity asymmetrically thus filling the half side quicker than the other half. This process increased the sloshing effect even further which is evident from the plot shown in the next figure. The velocity of the melt at extreme gates (1 and 4) can be seen to greater than the central gates (2 and 3).

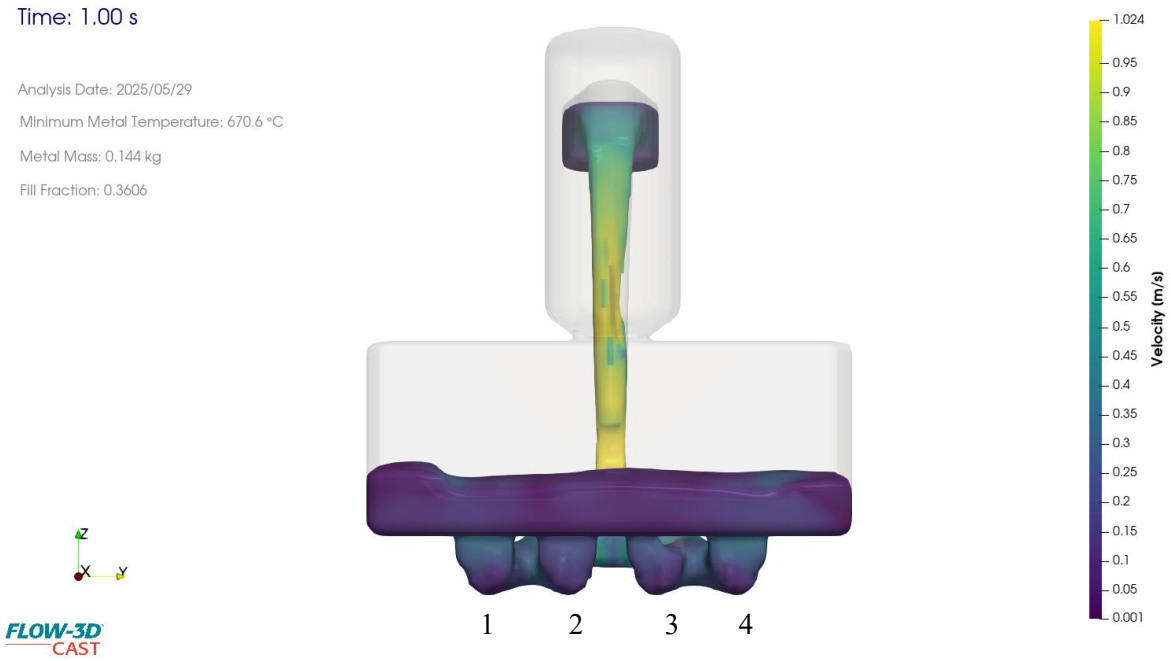

Figure 24 Gate View showing filling at time 1.0 sec for 4 ingates design with alternate filling Picture: Umar Siddique

The Figure 25 below shows the plot of average velocity at the 4 ingates for alternate filling system. It is evident that the whole plot is showing much transient behavior. There are major flow fluctuations in the start as the melt approach the ingates. For example at gate 1 the flow suddenly rose to 0.28 m/s and then drops to 0.1 m/s within $1/10^{th}$ of a second. Further it can be noted that flow started entering through the gate 3 at much later time and this delay led to more osciallations. Since each flow ingate has huge difference in initial approach velocity and times of approach, sloshing effect was much evident in this case which led to further flow oscillations. For example for gate 3 the flow rate dropped from 0.25 m/s to approximately 0.1 m/s in a short time period of 0.4 seconds ranging from 0.7 to 1.1 seconds. This drop affected the filling process significantly but introducing the sloshing effect later in the filling operation. Thus it can be seen

that this plot is showing more transient behavior than the conventionally designed 4 ingates filling system with sprue well.

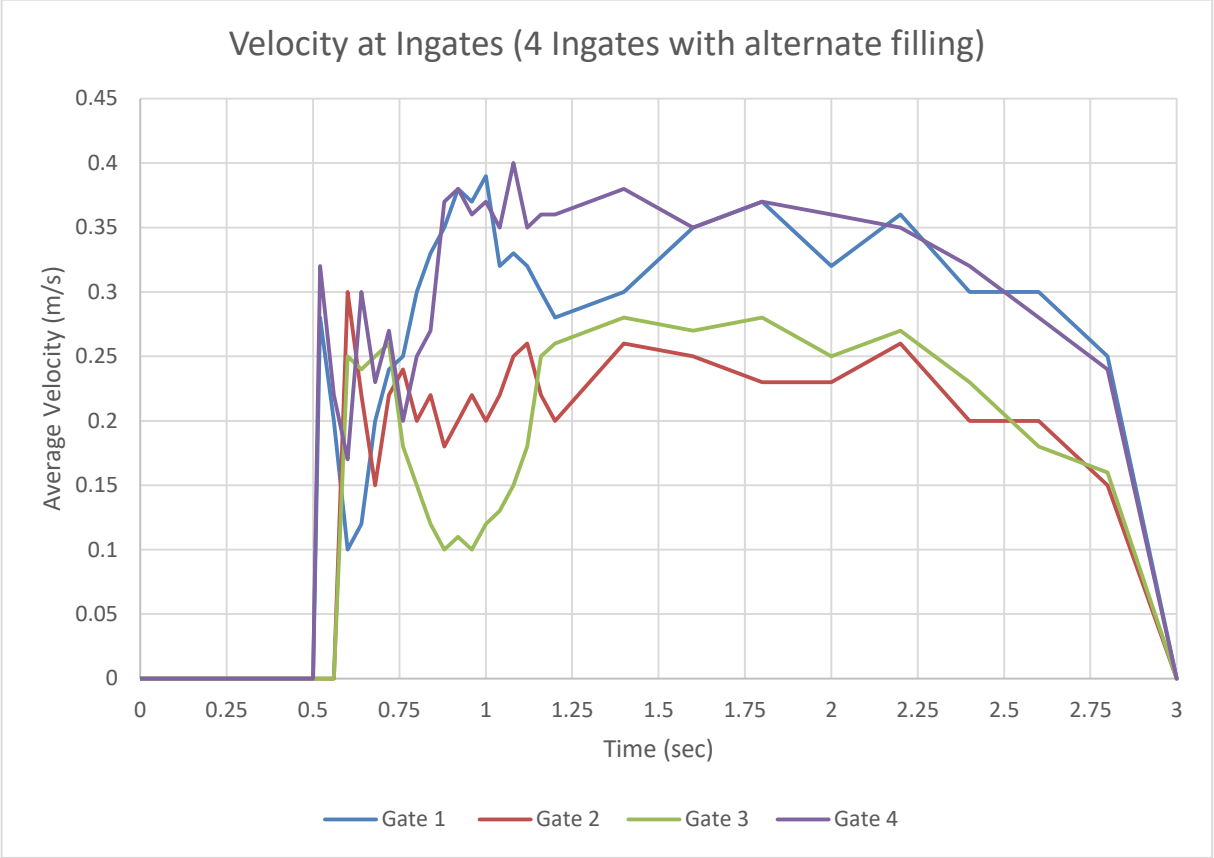

Figure 25 Plot showing average velocity with time at 4 ingates with alternate filling system Picture: Umar Siddique

5.2 Discussion

This section gives a detailed discussion of the result described in previous section. The goal of this was to determine if it was convenient to use higher filling rate while still minimizing the risk of part defects like air entrapment which eventually leads to porosity in solidified casted part. Lower filling time would lead to greater production rate and hence greater profits for casting foundries. To verify if this is possible, this simulation based study was conducted. The flow rate of the metal was increased as the number of ingates increased. Using multiple gating system with complex geometries has recently been possible with the use of additive manufacturing enabled sand molds. Following are some of the important discussion points.

- Higher melt input flow rate is possible by increasing the number of gates with the use of appropriate filling system.
- Inclusion of sprue well at the base of sprue has been observed as the most critical element in reducing the speed of the flow before entering the runner.
- Having multiple gates increases the chance of melt sloshing in the mold cavity and this can lead to air entrapment. This was observed in all the filling simulation cases. The transient flow behavior at the gates increased with the number of gates. Too much fluctuations were observed during the initial approach of the melt which attribute to sloshing effect in the mold cavity and the flow discontinuities earlier in the runner portion supplying the melt. Less transient behavior was observed during the later portion of filling process.
- In all the cases the velocity at the gates stayed under the critical limit of 0.5 m/s but flow discontinuities and transient behavior increased by the number of gates.
- The conventional 4 ingates filling system performed much better than the alternate filling system. Less transient flow behavior was observed from the velocity plots for conventional system than the alternate filling system. The presence of sprue well in case of conventional filling system proved essential in limiting the flow speed. The next section discusses the comparison of these filling system.

5.2.1 Comparison of Conventional vs. Alternate 4 Ingate Filling System

The conventional mold design with conical basin and sprue-well performed better in limiting the flow speed in the runner and caused less air entrapment in the mold cavity. This is evident from the analysis of void particles observed for both cases using Flow3d Post. The Figure 26 below shows the void particles in conventional model. The void particles refer to air bubbles which are entrapped in the part during the filling process. It can be seen that all the void particles are present on the top surface of mold cavity with no voids inside the part. This is critical, as the void particles inside the part cannot be removed while surface void particles can be removed easily using suitable surface finishing process. The sizes of void particles in this case vary from 1 to 1.6 mm. One important consideration to make is that increasing the volume and modulus of feeder can remove these voids but would also reduce the yield of the final castings and thus doesn’t seem to be a viable option as that would lead to more machining cost in the later

finishing of the product. Surface porosity is much easily manageable through appropriate machining technique.

Figure 26 Air bubbles shown as void particles for conventional 4 ingate filling system Picture: Umar Siddique

The Figure 27 below shows the void particles in the part casted using alternate filling system. There are void particle inside the mold cavity leading to porosity in the part. The void particles can be seen on the top surface of the mold cavity and in the centre region of the part. The reason for this is the fast speed of melt flow in the runner. The speed of the melt in case of conventional filling system design is around 0.7 m/s while for the alternate filling system the melt speed is 1.024 m/s. Further the flow discontinuities in case of the alternate filling system are much larger than conventional system. This was also observed from the slow influx of metal from gate 3 in case of alternate filling system. Hence it can be concluded that conventional conical sprue basin with sprue well performed better overall in reducing the filling time and maintaining the part quality by reducing the air entrapment.

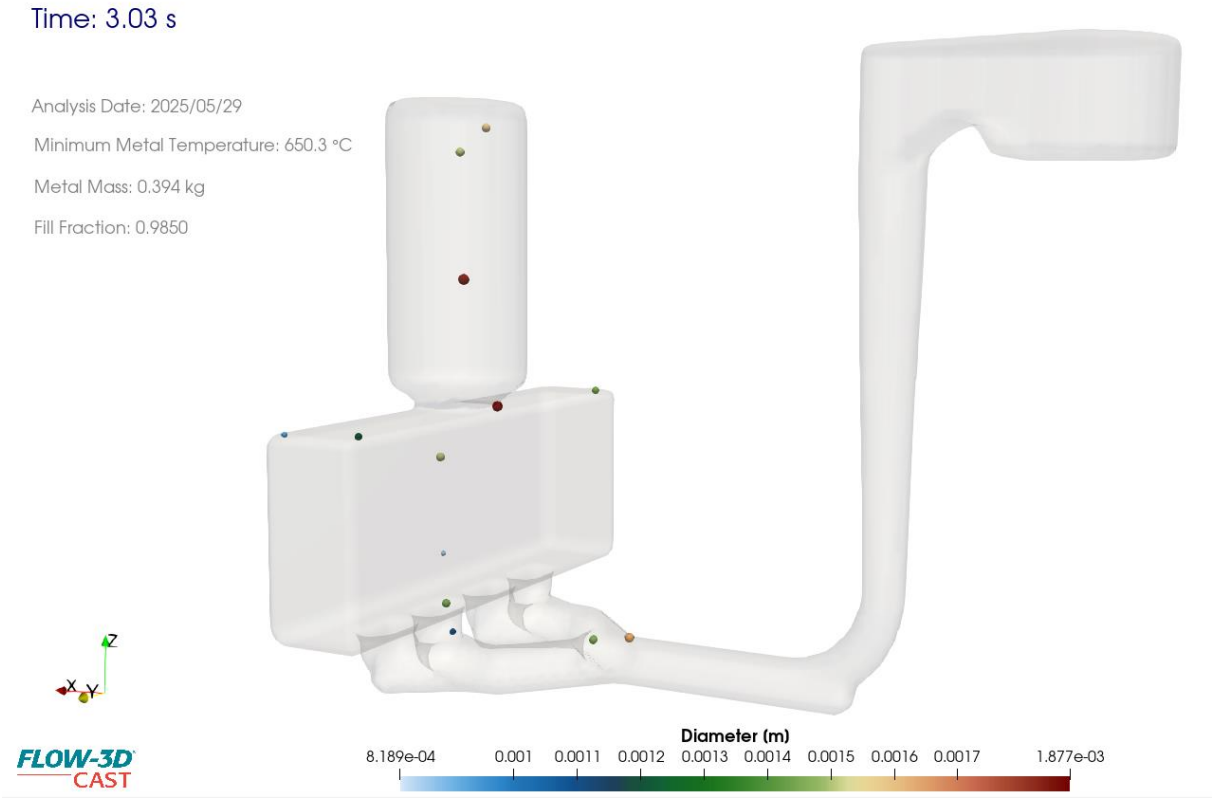

Figure 27 Air bubbles shown as void particles for alternate 4 ingate filling system Picture: Umar Siddique

5.2.2 Future Recommendations

This study focused effect of gating design on the melt velocity of the flow. The study was solely focused on the filling portion. Further insight and validation is needed to justify these results after the solidification phase. Further effect of gating design on the temperature changes of flow at the ingates needs to be studied. This will help to understand the formation of cold shuts in the part as the filling process from multiple gates might lead to different flow temperature at the gates. Other solidification defects like cracks, tears, blow holes etc can be noted by performing the cooling simulation.

6 Conclusions

The goal of this study was to determine the effect of number of gates on the melt flow velocity characteristics for AlSi10Mg alloy. This is one of the most common alloy with many applications in automotive, aerospace and medical applications. The study determined if it was feasible to increase the metal input flow rate so as to reduce the filling time of the molds thus increasing the production rate of foundries. Three cases were simulated for this purpose, with single ingate, 2 ingates and 4 ingates and a test case with alternate filling system. The 4 ingates filling system was simulated twice using a conventional filling system and alternate filling system to determine the better option. The conventional filling system consisted of a conical pouring basin with a straight tapered sprue and a sprue well provided at the end. The alternate filling system consisted of an offset basin with a tapered sprue with curve entrance to runner. The alternate filling system didn't have spure well at the end of sprue. After the velocity analysis done using Flow3dcast and observation of results using Flow3d Post it was found that conventional 4 ingate filling system performed best in reducing the filling speed while minimizing the air entrapment in the mold cavity.

References

[1] D.M. Stefanescu, A Succinct History of Metalcasting Knowledge, Inter Metalcast 17 (2023) 2373–2388. https://doi.org/10.1007/s40962-023-00971-5.

[2] Y. Kulkarni, Metal Casting Market Size, Share, and Trends 2025 to 2034, n.d.

[3] J. Campbell, Complete Casting Handbook: Metal Casting Processes, Techniques and Design, 2nd ed, Elsevier Science & Technology, Oxford, 2015.

[4] Rao, Metal casting: Principles and practice, 2003.

[5] O. Khayal, CLASSIFICATIONS OF MANUFACTURING PROCESSES AND STRATEGY USED IN SELECTING SUITABLE PROCESSES FOR SUITABLE APPLICATIONS, (2019). https://doi.org/10.13140/RG.2.2.36275.17447.

[6] G. Gyarmati, L. Bogoly, M. Stawarz, G. Fegyverneki, Z. Kéri, M. Tokár, T. Mende, Grain Refiner Settling and Its Effect on the Melt Quality of Aluminum Casting Alloys, Materials 15 (2022) 7679. https://doi.org/10.3390/ma15217679.

[7] T. Bogdanoff, M. Tiryakioglu, A.E.W. Jarfors, E. Ghassemali, A simple procedure to assess the Complete Melt Quality in aluminium castings: implementation in a die-casting and a rheo-casting, International Journal of Cast Metals Research 37 (2024) 71–79. https://doi.org/10.1080/13640461.2023.2293415.

[8] S. Chakravarti, S. Sen, An investigation on the solidification and porosity prediction in aluminium casting process, J. Eng. Appl. Sci. 70 (2023) 21. https://doi.org/10.1186/s44147-023-00190-z.

[9] A.H. Fazeli, H. Saghafian, S.M.A. Boutorabi, J. Campbell, The Fluidity of Aluminium Ductile Irons, Inter Metalcast 16 (2022) 143–152. https://doi.org/10.1007/s40962-021-00581-z.

[10] Y. Xiao, C. Xiao, D. Chang, Y. Ji, B. Wang, F. Li, D. Wang, B. Sun, Time-varying disturbances of temperature field in investment casting and corresponding shrinkage defects control methods, Journal of Materials Research and Technology 35 (2025) 5147–5159. https://doi.org/10.1016/j.jmrt.2025.02.164.

[11] K.D. Carlson, C. Beckermann, Prediction of Shrinkage Pore Volume Fraction Using a Dimensionless Niyama Criterion, Metall Mater Trans A 40 (2009) 163–175. https://doi.org/10.1007/s11661-008-9715-y.

[12] A. Reis, Z. Xu, R.V. Tol, R. Neto, Modelling feeding flow related shrinkage defects in aluminum castings, Journal of Manufacturing Processes 14 (2012) 1–7. https://doi.org/10.1016/j.jmapro.2011.05.003.

[13] Z. Chen, Y. Li, F. Zhao, S. Li, J. Zhang, Progress in numerical simulation of casting process, Measurement and Control 55 (2022) 257–264. https://doi.org/10.1177/00202940221102656.

[14] S.V. Patankar, D.B. Spalding, A computer model for three-dimensional flow in furnaces, Symposium (International) on Combustion 14 (1973) 605–614. https://doi.org/10.1016/S0082-0784(73)80057-8.

[15] J. Welch, F. Harlow, J. Shannon, B. Daly, THE MAC METHOD-A COMPUTING TECHNIQUE FOR SOLVING VISCOUS, INCOMPRESSIBLE, TRANSIENT FLUID-FLOW PROBLEMS INVOLVING FREE SURFACES, 1965. https://doi.org/10.2172/4563173.

[16] C.W. Hirt, B.D. Nichols, Volume of fluid (VOF) method for the dynamics of free boundaries, Journal of Computational Physics 39 (1981) 201–225. https://doi.org/10.1016/0021-9991(81)90145-5.

[17] H. Qiang, Z. Shan, H. Yang, W. Song, Y. Sun, L. Liu, High-Performance 3D Sand Printing Process Using Interlayer Heating, Additive Manufacturing Frontiers 3 (2024) 200154. https://doi.org/10.1016/j.amf.2024.200154.

[18] E.S. Almaghariz, B.P. Conner, L. Lenner, R. Gullapalli, G.P. Manogharan, B. Lamoncha, M. Fang, Quantifying the Role of Part Design Complexity in Using 3D Sand Printing for Molds and Cores, Inter Metalcast 10 (2016) 240–252. https://doi.org/10.1007/s40962-016-0027-5.

[19] M. Wänerholm, Nordic Foundries: Best Available Techniques (BAT), Nordic Council of Ministers, Copenhagen K, 2017. https://doi.org/10.6027/TN2017-562.

[20] R.G. Chougule, B. Ravi, Casting cost estimation in an integrated product and process design environment, International Journal of Computer Integrated Manufacturing 19 (2006) 676–688. https://doi.org/10.1080/09511920500324605.
[21] B. Denkena, J.T. Schürmeyer, R. Kaddour, V. Böß, Assessing mould costs analysing manufacturing processes of cavities, Int J Adv Manuf Technol 56 (2011) 943–949. https://doi.org/10.1007/s00170-011-3265-y.
[22] A. Fiorentino, Cost drivers-based method for machining and assembly cost estimations in mould manufacturing, Int J Adv Manuf Technol 70 (2014) 1437–1444. https://doi.org/10.1007/s00170-013-5419-6.
[23] I. Iraola-Arregui, H. Ben Youcef, V. Trabadelo, Cost Estimation Tool for Metallic Parts Made by Casting: A Case Study, Metals 13 (2023) 216. https://doi.org/10.3390/met13020216.
[24] M. Sajid, A. Wasim, S. Hussain, M. Jahanzaib, Manufacturing feature-based cost estimation of cast parts, China Foundry 15 (2018) 464–469. https://doi.org/10.1007/s41230-018-8084-4.
[25] M. Sortino, B. Motyl, G. Totis, Preventive evaluation of mould production cost in aluminium casting, Int J Adv Manuf Technol 70 (2014) 285–295. https://doi.org/10.1007/s00170-013-5273-6.
[26] A. Martof, R. Gullapalli, J. Kelly, A. Rea, B. Lamoncha, J.M. Walker, B. Conner, E. MacDonald, Economies of Complexity of 3D Printed Sand Molds for Casting, (2018). https://doi.org/10.26153/TSW/17003.
[27] D. Joshi, B. Ravi, Quantifying the Shape Complexity of Cast Parts, Computer-Aided Design and Applications 7 (2010) 685–700. https://doi.org/10.3722/cadaps.2010.685-700.
[28] N. Anwar, Inorganic foundry binders for sustainable sand molding, Aalto University, 2024.
[29] I. Vasková, D. Fecko, P. Delimanová, L. Jankovčin, M. Hrubovčáková, Influence of Shape of Gating System on Pouring Time and Filling of a Sprue with the Use of MAGMA5 Optimization, Archives of Metallurgy and Materials (2024) 1131–1136. https://doi.org/10.24425/amm.2024.150934.
[30] K. Taki, G. Endo, Y. Maeda, Molten Aluminum Alloy Flow through Casting Filter Installed at Sprue, Inter Metalcast 17 (2023) 2477–2483. https://doi.org/10.1007/s40962-023-00976-0.
[31] S.R. Sama, T. Badamo, P. Lynch, G. Manogharan, Novel sprue designs in metal casting via 3D sand-printing, Additive Manufacturing 25 (2019) 563–578. https://doi.org/10.1016/j.addma.2018.12.009.
[32] K. Munpakdee, P. Ninpetch, S. Otarawanna, R. Canyook, P. Kowitwarangkul, Effect of feed sprue size on porosity defects in Platinum 950 centrifugal investment casting via numerical modelling, IOP Conf. Ser.: Mater. Sci. Eng. 1137 (2021) 012021. https://doi.org/10.1088/1757-899X/1137/1/012021.
[33] Md.A.-A. Sarkar, M. Rahman, M.K. Alam, A.N.Md. Abdullah, M.Md. Anisuzzaman, Effect of Sprue Design in Nickel-Chromium Cast Crown Margin, Pesqui. Bras. Odontopediatria Clín. Integr. 21 (2021) e0110. https://doi.org/10.1590/pboci.2021.022.
[34] P.J. Brockhurst, V.G. McLaverty, Z. Kasloff, A castability standard for alloys used in restorative dentistry, Oper Dent 8 (1983) 130–139.
[35] D. Chan, V. Guillory, R. Blackman, K. Chung, The effects of sprue design on the roughness and porosity of titanium castings, The Journal of Prosthetic Dentistry 78 (1997) 400–404. https://doi.org/10.1016/S0022-3913(97)70048-9.
[36] Chan, Blackman, Kaiser, Chung, The effect of sprue design on the marginal accuracy of titanium castings, J of Oral Rehabilitation 25 (1998) 424–429. https://doi.org/10.1046/j.1365-2842.1998.00268.x.
[37] M.B. Leal, S.M. Paulino, V.O. Pagnano, O.L. Bezzon, Influence of investment type and sprue number on the casting accuracy of titanium crown margins, The Journal of Prosthetic Dentistry 95 (2006) 42–49. https://doi.org/10.1016/j.prosdent.2005.11.004.
[38] M.H. Raza, A. Wasim, M. Sajid, S. Hussain, Investigating the effects of gating design on mechanical properties of aluminum alloy in sand casting process, Journal of King Saud University - Engineering Sciences 33 (2021) 201–212. https://doi.org/10.1016/j.jksues.2020.03.004.

[39] M. Bruna, M. Galčík, Effect of Filter Type on Mechanical Properties During Aluminium Alloy Casting, Archives of Foundry Engineering (2022) 95–98. https://doi.org/10.24425/afe.2022.140241.
[40] Anjo, Victor, R. khan, Gating system design for casting thin aluminium alloy (Al-Si) plates, Leonardo Electronic Journal of Practices and Technologies 23 (n.d.) 51–62.
[41] Mohd. Bilal Naim Shaikh, S. Ahmad, A. Khan, M. Ali, Optimization of Multi-Gate Systems in Casting Process: Experimental and Simulation Studies, IOP Conf. Ser.: Mater. Sci. Eng. 404 (2018) 012040. https://doi.org/10.1088/1757-899X/404/1/012040.
[42] R. Dojka, J. Jezierski, J. Campbell, Optimized Gating System for Steel Castings, J. of Materi Eng and Perform 27 (2018) 5152–5163. https://doi.org/10.1007/s11665-018-3497-1.
[43] D. Vaghasia, Gating System Design Optimization for Sand Casting, Indian Institute of Technology Bombay, 2009.
[44] giessereilexikon lexicon, Slag inclusions, Foundary Lexicon (n.d.).
[45] M.M. Shuvo, M. Skiadopoulos, K.S. Shahed, T. Badamo, P. Shokouhi, R. Voigt, G. Manogharan, An Integrated Computational and Experimental Study of Vortex Chamber Performance for Reducing Entrapped Slag and Reoxidation Defects in Steel Castings, Inter Metalcast (2025). https://doi.org/10.1007/s40962-025-01598-4.
[46] Y. Wang, S. Yang, F. Wang, J. Li, Optimization on Reducing Slag Entrapment in 150 × 1270 mm Slab Continuous Casting Mold, Materials 12 (2019) 1774. https://doi.org/10.3390/ma12111774.
[47] R. Donahue, R. Hardin, C. Beckermann, Modeling of oxide inclusions in steel casting, IOP Conf. Ser.: Mater. Sci. Eng. 1281 (2023) 012035. https://doi.org/10.1088/1757-899X/1281/1/012035.
[48] S.H. Majidi, Modeling of air entrainment and oxide inclusion formation during pouring of metal castings, Doctor of Philosophy, University of Iowa, 2018. https://doi.org/10.17077/etd.kn8u-4us3.
[49] D. Dispinar, J. Campbell, Porosity, hydrogen and bifilm content in Al alloy castings, Materials Science and Engineering: A 528 (2011) 3860–3865. https://doi.org/10.1016/j.msea.2011.01.084.
[50] Heine, Loper, Rosenthal, Principles of Metal Casting, 2nd ed., McGraw-Hill, 1967.